

High temperature reactions of individual nanoparticles

Abigail M. Friese, Audrey R. Burrows, Chris Lau, and Scott L. Anderson

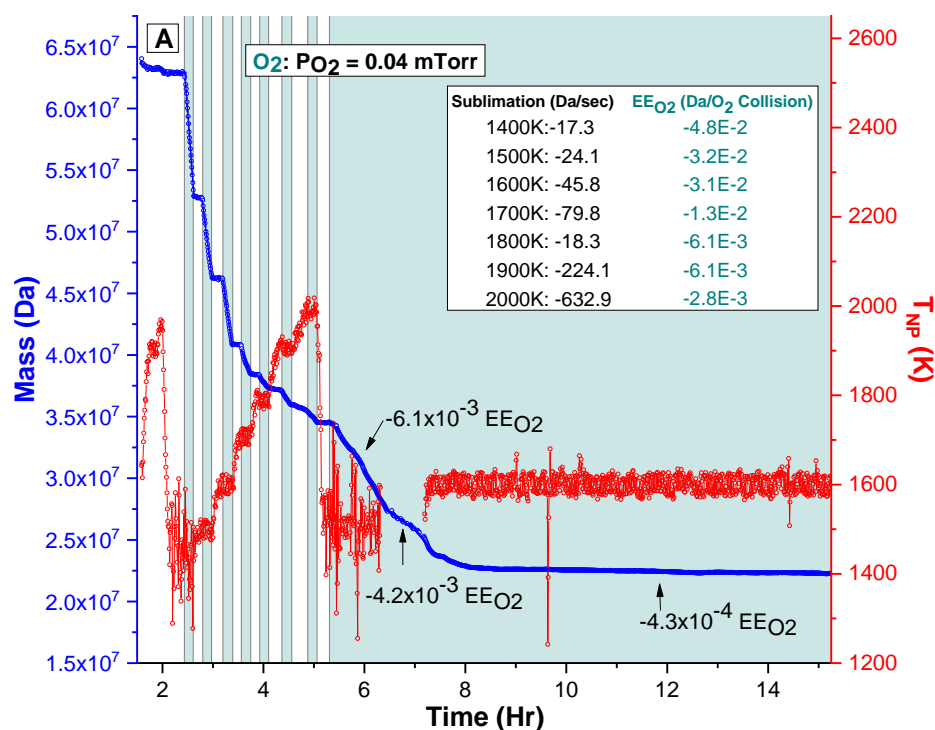
Chemistry Dept, University of Utah, Salt Lake City, UT 84112, USA. anderson@chem.utah.edu

ABSTRACT

Understanding structure-reactivity relationships for nanoparticles (NPs) is complicated by the fact that each NP has a different distribution of surface sites, and by the evolution of the NP structure as reactions add or remove material. We have developed a single NP mass spectrometry method that allows the absolute kinetics for gas-surface reactions of individual NPs to be measured as a function to time, while varying NP temperature and gas pressure/composition, with or without various pre-treatments such as melting or heating to drive sublimation or composition changes for the surface layer.

A single nanoparticle (NP) of the material of interest is electrodynamically trapped in either inert or reactive atmospheres, and laser heated to a temperature of interest, which is measured by fitting the particle's thermal emission spectrum. Kinetics for mass-changing processes such as sublimation, oxide formation, and addition or etching reactions, are measured by simply tracking the NP mass vs. time as the reaction proceeds. By monitoring reactivity over time, the effects of evolution of the surface (passivation, roughening, etc.) can be followed, and comparing results for different NPs provides insights into the effects of NP heterogeneity on reactivity. The upper temperature limit for the experiment is determined only by the sublimation kinetics of the NPs, thus for refractory materials, kinetics can be measured to temperatures above 3000 K. For materials with modest vapor pressure at their melting points, chemistry can also be studied for molten nanodroplets.

The method will be illustrated with results for O₂ oxidation and sublimation of silicon ($T_{\text{melt}} = 1687$ K) and hafnium carbide, HfC ($T_{\text{melt}} = 4170$ K). The figure shows one type of experiment, in which a HfC NP was trapped, cleaned by preheating to 1900 K in argon (white background), then subjected to a temperature ramp from 1400 K to 2000 K, measuring both the sublimation rates in argon (white background) and the etching rates in O₂ (aqua background). The slope of the



mass vs. time plot gives the absolute mass loss rates (Da/sec), and it can be seen that the sublimation rates increased as the temperature increased, but that the O₂ etching rates decreased, due to partial passivation of the NP surface. The second part of the experiment followed the NP mass for >~10 hours at constant O₂ pressure with T_{NP} initially at 1500 K, then at 1600 K. Here, the NP passivated, with kinetics slowing by two orders of magnitude. By comparing experiments at different temperatures and pressures, it is possible to map out how the etching, sublimation, and passivation kinetics vary with reaction conditions.

Simulating the Anion Photoelectron Spectrum of Tetrazolyl with the Time-Independent Multimode Vibronic Coupling Approach

Chris Avanesian and David R. Yarkony

Department of Chemistry, Johns Hopkins University, Baltimore, MD, USA

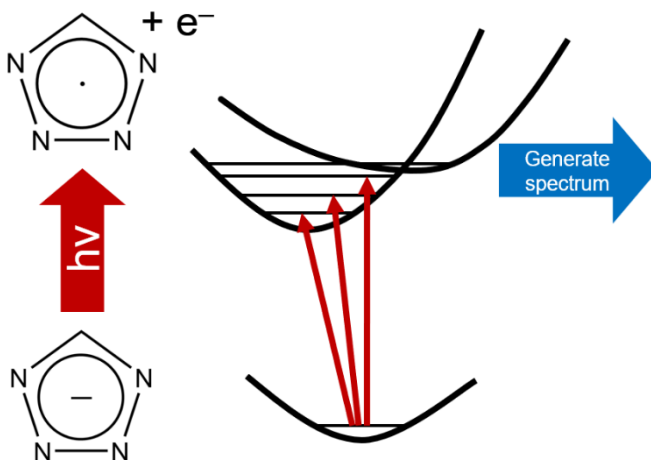
Email: cavanese1@jhu.edu

ABSTRACT

Tetrazolyl has recently shown promise as the basis of high-energy-density materials.^{1,2} It is an azolyl ($N_x(CH)_y$; $x + y = 5$), a class of 35-electron neutral radicals which are substitutional isomers of cyclopentadienyl. The high D_{5h} symmetry of cyclopentadienyl results in its electronic ground state being doubly degenerate, having ${}^2E_1'$ symmetry.³ This has consequences for the closely-related potential energy surface (PES) of tetrazolyl, which has a conical intersection seam between its two lowest-energy electronic states, near the ground state equilibrium geometry.

The present work aims to simulate the anion ultraviolet photoelectron spectrum of tetrazolyl. A quasidiabatic Hamiltonian is used with a time-independent multimode vibronic coupling approach to yield the vibronic eigenstates and, by extension, the spectral intensity distribution.⁴ Most applications of this approach only include up to quadratic terms in the Hamiltonian, but this is expected to be insufficient, so quartic terms will be included.^{3,5}

Ab initio electronic structure calculations are performed using the COLUMBUS suite of electronic structure codes. This consists of the multi-configurational self-consistent field method followed by multireference configuration interaction with single and double excitations and generalized interacting space restrictions. Dunning's cc-pVDZ basis set is used for the neutral radical. Geometry optimizations were performed, which identified, among others, three key critical points. Minima were found on the ground and first electronic excited states, both having C_{2v} symmetry. In addition, a minimum energy crossing (MEX) was found between these states. The quasidiabatic Hamiltonian will be generated using a variant of Surfgen (produces coupled PESs by fitting to provided *ab initio* points) for bound systems, and NadVibS (nonadiabatic vibrational spectrum simulation package) will be used to simulate the spectrum.



¹ Piekiet, N. and Zachariah, M. R. Decomposition of Aminotetrazole Based Energetic Materials under High Heating Rate Conditions. *J. Phys. Chem. A* 116, 1519-1526, 2012.

² Klapötke, T. M. and Stierstorfer, J., in *Green Energetic Materials*, ed. Brinck, T., John Wiley & Sons, Ltd.: Chichester, United Kingdom, 133-177, 2014.

³ Dillon, J., Yarkony, D. R., and Schuurman, M. S. On the construction of quasidiabatic state representations of bound adiabatic state potential energy surfaces coupled by accidental conical intersections: Incorporation of higher order terms. *J. Chem. Phys.* 134, 044101, 2011.

⁴ Köppel, H., Domcke, W., and Cederbaum, L. S., in *Conical Intersections: Electronic Structure, Dynamics & Spectroscopy*, eds. Domcke, W., Yarkony, D. R., and Köppel, H., World Scientific Publishing Co. Plte. Ltd.: Toh Tuck Link, Singapore, 323-367, 2004.

⁵ Dillon, J., Yarkony, D. R., and Schuurman, M. S. On the simulation of photoelectron spectra complicated by conical intersections: Higher-order effects and hot bands in the photoelectron spectrum of triazolide $(CH)_2N_3^-$. *J. Chem. Phys.* 134, 184314, 2011.

Controlling the unimolecular dissociation rate of an ultracold reaction

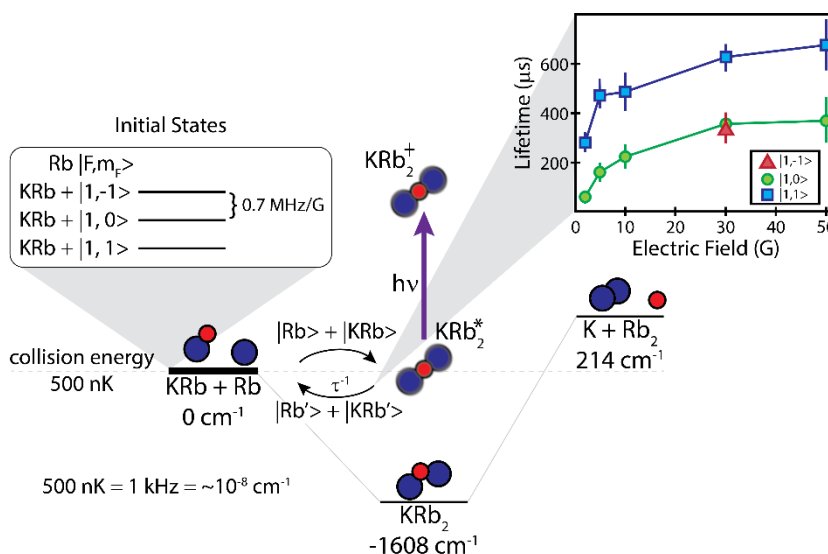
Mark C. Babin,^{a,b} Lingbang Zhu,^{a,b} Yi-Xiang Liu^{a,b} and Kang-Kuen Ni^{a,b,c}^a Department of Chemistry and Chemical Biology, Harvard University, Cambridge, Massachusetts 02138, USA. Email: markbabin@g.harvard.edu^b Harvard-MIT Center for Ultracold Atoms, Cambridge, Massachusetts 02138, USA^c Department of Physics, Harvard University, Cambridge, Massachusetts 02138, USA

ABSTRACT

Transient intermediate reaction complexes connect reactants and products along the reaction path, controlling not only the overall reaction rate but also the dynamics of chemical transformation. While transient in nature, the lifetime of these species can be extended from a few vibrational periods, on the order of picoseconds, to the nanosecond or even millisecond timescale when prepared under ultracold conditions ($T < 1 \mu\text{K}$).^{1,2} Here, we show that this extension in lifetime can be actively controlled in the endothermic $\text{KRb} + \text{Rb} \leftrightarrow \text{KRb}_2$ reaction at 500 nK not only by judicious choice

of reactant state, but also by external magnetic fields. In our experiment, a bulk gas of ultracold KRb molecules in a single hyperfine level of their ground rovibronic state and Rb atoms in their ground hyperfine ($F = 1$) level are prepared and trapped in an optical dipole trap. The hyperfine levels of both KRb and Rb can be controlled coherently, allowing for molecular and atomic state preparation with near-unit fidelity. Stochastic reactive collisions are initiated upon formation of the atom-molecule

cloud and measurements of the KRb_2 collisional complex lifetime, the inverse of its unimolecular dissociation rate, are performed by single-photon UV ionization and subsequent ion-imaging. Despite the stochastic nature of these collisions, we have previously observed that our optical trapping light rapidly photoexcites these complexes,² allowing us to set a clear starting time of these dynamics by shutting off the trapping light and probing at various delay times. We interrogate myriad reactant state combinations, as well as various external electric and magnetic fields, revealing that the dissociation rate of KRb_2 can be controlled continuously by over an order of magnitude and is relatively insensitive to the initial molecular hyperfine state. As the first demonstration of control over a unimolecular reaction, this work is a crucial step towards an era of fully-controlled chemistry.

¹ M.-G. Hu, *et al.* Direct Observation of Bimolecular Reactions of Ultracold KRb. *Science* 366, 1111, 2019.² M. A. Nichols, *et al.* Detection of Long-Lived Complexes in Ultracold Atom-Molecule Collisions. *Phys. Rev. X* 22, 011049, 2022.

Stereodynamical control of cold collisions between two aligned D₂ molecules

P. G. Jambrina,^a J. F. E. Croft,^b J. Zuo,^c H. Guo,^c F. J. Aoiz^d and N. Balakrishnan^e

^a*Departamento de Química Física, Universidad de Salamanca, Salamanca 37008, Spain*

^b*The Dodd-Walls Centre for Photonic and Quantum Technologies, Dunedin, New Zealand and Department of Physics, University of Otago, Dunedin, New Zealand*

^c*Department of Chemistry and Chemical Biology, University of New Mexico, Albuquerque, New Mexico 87131, USA*

^d*Departamento de Química Física, Universidad Complutense, Madrid 28040, Spain*

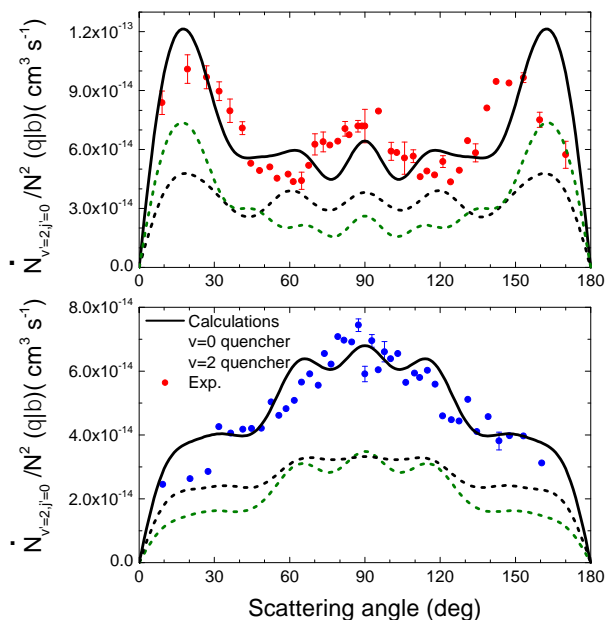
^e*Department of Chemistry and Biochemistry, University of Nevada, Las Vegas, Nevada 89154, USA.
E-mail: naduvala@unlv.nevada.edu*

ABSTRACT

Bimolecular collisions involving diatomic molecules are topics of active investigation due to the continuing interest in cooling and trapping of molecules and their applications in sensing, precision spectroscopy, quantum information processing, and ultracold chemistry, to name a few. By combining optical state-preparation using the Stark-induced adiabatic Raman passage (SARP) method with co-expansion of the colliding species in the same molecular beam Mukherjee and coworkers have been able to explore the stereodynamics of atom-molecule and molecule-molecule collisions at collision energies in the vicinity of 1 K¹. In this regime, collision outcomes are dominated by isolated partial waves allowing measurements of differential cross sections (DCSs) with partial wave resolution.

Recently, Mukherjee and coworkers have reported DCS for collisions between two aligned D₂ molecules prepared in the $v=2$ vibrational level and $j=2$ rotational level using the SARP method. They attributed key features of the angular distributions to a $l=2$ partial wave resonance in the incident channel.

Here we provide a first principles simulation of the experiment using explicit quantum close-coupling calculations². Our calculations take both aligned-aligned collisions of D₂ molecules in the $v=2$ vibrational level as well as collisions between state-prepared D₂ in $v=2$ and unprepared D₂ in $v=0$ that are present in the experiment. As shown in the Figure our calculations using a full-dimensional interaction potential for the H₂+H₂ system nearly quantitatively reproduces the experimental angular distribution for both H-SARP and V-SARP preparations. However, a key difference is that our calculations show that the DCS is dominated by a $l=4$ shape resonance than a $l=2$ resonance ascribed in the experiment.



¹ Zhou, H., Perreault, W. D., Mukherjee, N. and Zare, R. N. Anisotropic dynamics of resonant scattering between a pair of cold aligned diatoms. *Nat. Chem.* 14, 658-663, 2022

² Jambrina, P. G., Croft, J. F. E., Zuo, J., Guo, H., Balakrishnan, N. and Aoiz, F. J. Stereodynamical Control of Cold Collisions between Two Aligned D₂ Molecules. *Phys. Rev. Lett.* 130, 033002, 2023

Long-Range-Fit: A program to fit long-range interactions

Adrian Batista-Planas, Ernesto Quintas-Sánchez and Richard Dawes

Department of Chemistry, Missouri University of Science and Technology, Rolla, MO 65409-0010

Email: albgzz@mst.edu

ABSTRACT

Long-range molecular interactions play an essential role in atmospheric and environmental chemistry, astrochemistry, and many other relevant fields. For modeling purposes, these interactions can be better understood by constructing a potential energy surface (PES) for the system of interest.¹ The contributing interactions in the long-range region of a PES (namely electrostatic, induction, dispersion, ...) are usually evaluated by perturbation theory techniques after expanding the electronic charge distribution in the well-known multipolar series.² However, although its theoretical description is a well-studied subject, the implementation of its mathematical formulation can be extremely challenging, considering that the analytical expressions (which can be written as a sum of terms for each of the different interactions) could be several pages long of explicit algebra just for a single term and changes from system to system. Our program “Long-Range-Fit” (LRF), is an interactive user-friendly interface designed to assist in fitting the long-range region of a PES for systems composed of (any) two rigid molecules. Once the symmetry of each of the fragments is specified, LRF is programmed to automatically generate and fit the corresponding analytical expressions for the most common symmetry groups (up to the desired order of accuracy, defined by the maximum order in the expansion of each interaction, also specified by the user). LRF is designed to complement programs such as AUTOSURF³ in providing a more robust and accurate representation in the long-range region of a PES.

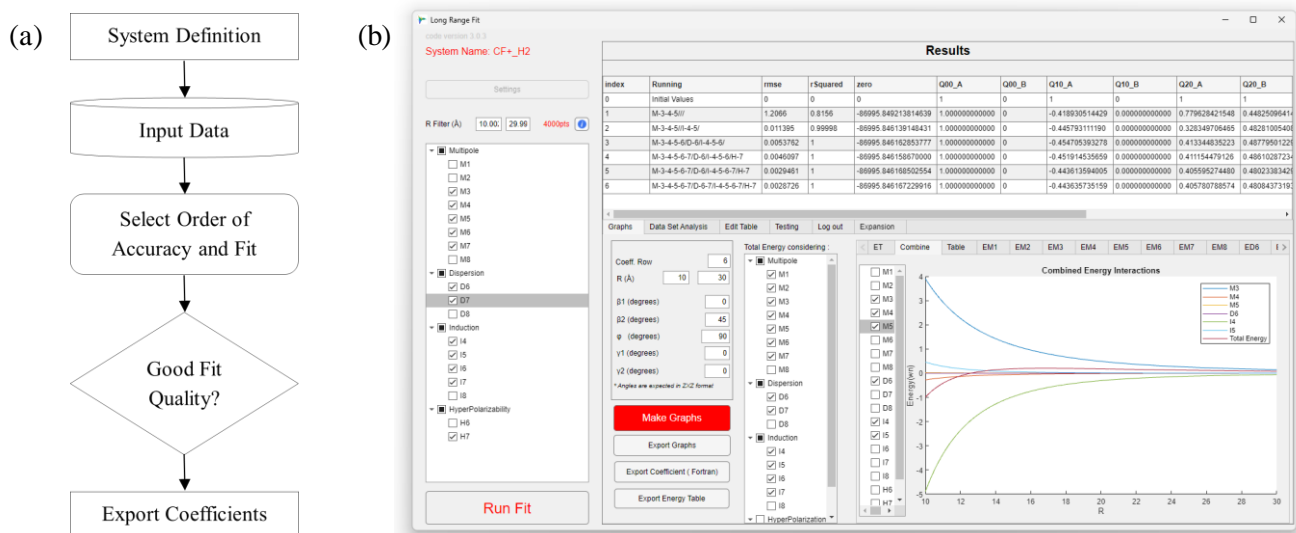


Figure 1: (a) LRF flowchart: The program starts with the “System Definition” (specifying each molecule by symmetry group, net charge, and some initial coefficient values such as the charge and/or dipole, if known) and reading in the *ab initio* data to be fit. Once the order of accuracy (order in the expansion of each interaction) is selected by the user, LRF generates the corresponding analytical expression and performs a fit. Finally, the fit quality is analyzed to decide whether the fit has converged and is good enough to be used. (b) LRF main control window.

¹ R. Dawes and E. Quintas-Sánchez, The Construction of Ab Initio-Based Potential Energy Surfaces. *Rev. Comp. Chem.*, vol. 31, ed. Abby L. Parrill and Kenny B. Lipkowitz, ch. 5, pp. 199-256, 2018.

² A. Stone, *The Theory of Intermolecular Forces*, 2nd ed., Oxford University Press, United Kingdom, 2013.

³ E. Quintas-Sánchez and R. Dawes, AUTOSURF: A Freely Available Program to Construct Potential Energy Surfaces. *J. Chem. Inf. Model.* 59, 262-271, 2019.

Gas Phase Infrared Investigation of the Water Catalyzed Isomerization of N1- to N6-Methyl-Adenosine

James Raymon Breton,^a Fabian Menges,^a Sigrid Nachtergaele^b and Mark Albert Johnson^a

^a Johnson Lab, Chemistry Department, Yale University, 225 Prospect St, New Haven, CT 06511, USA. Email: james.breton@yale.edu

^bNachtergaele Lab, Department of Molecular, Cellular, and Developmental Biology, Yale University

ABSTRACT

Protonated 1-methyladenosine (m^1A+H^+) and 6-methyladenosine (m^6A+H^+) are naturally occurring molecules that play important roles in RNA chemistry.^{1,2,3} Previous studies demonstrated that isomerization between m^1A and m^6A occurs most efficiently at pH values between 8-9.⁴ This dependence was rationalized by invoking an initial isomerization step where hydroxide attacks the m^1A scaffold at either the C₂ or C₆ position.⁴ The Dimroth rearrangement⁴ was the mechanism proposed for this isomerization, and Engel⁵ later demonstrated using NMR spectroscopy and isotopically labeled (¹⁵N) nitrogen that methyladenosine does in fact undergo the ring opening mechanism as indicated in Figure 1. Here we explore a mechanism that involves a nucleophilic attack by hydroxide at the 6-membered pyrimidine ring of m^1A+H^+ (between ring positions 1 and 2). This would lead to a ring-opening that allows for a rotation around the C₅-C₆ bond. Subsequent ring closure with loss of hydroxide would then yield the m^6A+H^+ product. While this mechanism is known, we aim to capture and structurally characterize key reaction intermediates utilizing cryogenic ion chemistry and isomer-selective vibrational spectroscopy to reaffirm the current isomerization mechanism. We will report high-resolution mass spectra and cryogenic vibrational spectra of m^1A+H^+ , m^6A+H^+ ($m/z = 282$ Da), and the proposed reaction intermediate corresponding to the stoichiometry $m^{\ddagger}A+H^++H_2O$ ($m/z = 300$ Da). Preliminary results indicate that a species at $m/z=282$ Da (which could be m^1A+H^+ or m^6A+H^+) can be generated upon collisional activation of the 300 Da intermediate. The implications of these findings on the isomerization mechanism will be discussed in the context of the computed potential energy barriers and structures of the transition states.

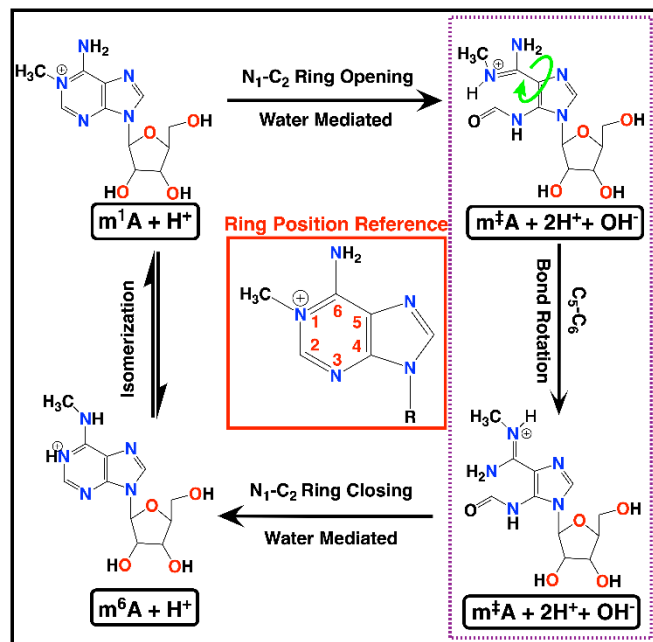


Figure 1: Proposed m^1A+H^+/m^6A+H^+ isomerization reaction pathway, with ring position reference in center of figure.

¹ Ratel, D.; Ravanat, J. L.; Berger, F.; Wion, D. N6-methyladenine: the other methylated base of DNA. *Bioessays* 28(3), 309-315, 2006.

² Kamat, S. S.; Fan, H.; Sauder, J. M.; Burley, S. K.; Shoichet, B. K.; Sali, A.; Raushel, F. M. Enzymatic deamination of the epigenetic base N-6-methyladenine. *Journal of the American Chemical Society* 133 (7), 2080-2083, 2011.

³ Hori, H. Methylated nucleosides in tRNA and tRNA methyltransferases. *Frontiers in genetics* 5, 144, 2014.

⁴ Macon, J. B.; Wolfenden, R. 1-Methyladenosine. Dimroth rearrangement and reversible reduction. *Biochemistry* 7 (10), 3453-3458, 1968.

⁵ Engel, J. D. Mechanism of the Dimroth rearrangement in adenosine. *Biochemical and biophysical research communications* 64 (2), 581-586, 1975.

Crossed-Beam Studies of the O(³P, ¹D) Reactions with Cyanoacetylene and Cyanoethylene: Product branching Fractions and Role of Intersystem-Crossing

Giacomo Pannacci,^a Gianmarco Vanuzzo,^a Luca Mancini,^a Pengxiao Liang,^a Demian Marchione,^a Marzio Rosi,^b Nadia Balucani^a and Piergiorgio Casavecchia^a

^aDepartment of Chemistry, Biology and Biotechnologies, University of Perugia, 06123 Perugia, Italy

^bDept. Environmental and Civil Engineering, Università di Perugia, 06125 Perugia, Italy

Email: piergiorgio.casavecchia@unipg.it

ABSTRACT

Cyanoacetylene (HCCCN) and cyanoethylene (acrylonitrile) (CH₂CHCN) are of considerable interest in astrochemistry being ubiquitous in space (molecular clouds, solar-type protostars, circumstellar envelopes) and also relatively abundant. They are also abundant in the upper atmosphere of Titan. Since oxygen is the third most abundant element in the universe, the reaction O(³P) with these two nitriles can be of relevance in the chemistry of extraterrestrial environments. In addition, the oxidation of cyanocacetylene and acrylonitrile is also relevant in combustion environments, because the thermal decomposition of pyrrolic and pyridinic structures present in fuel-bound nitrogen generates many nitrogen-bearing compounds, including cyanoacetylene and acrylonitrile. Despite their relevance, limited information exists on the reactions of oxygen atoms with these important nitriles. Here, we report on a combined experimental and theoretical investigation of the reactions of cyanoacetylene and acrylonitrile with both ground ³P and excited ¹D atomic oxygen. From product angular and time-of-flight distributions in crossed molecular beam experiments with mass spectrometric detection at the collision energy of about 31 kJ/mol, we have identified the primary reaction products and determined their branching fractions (BFs). Theoretical calculations of the relevant triplet and singlet potential energy surfaces (PESs) were performed to assist the interpretation of the experimental results and elucidate the reaction mechanisms. Adiabatic statistical calculations of product BFs for the decomposition of the main triplet and singlet intermediates were carried out. Combining the experimental and theoretical results, we have reached the following conclusions. (i) The O(³P)+HCCCN reaction exhibits a minor adiabatic channel leading to OCCCN(cyanoketyl)+H (BF=0.10±0.05), while the dominant channel (BF=0.90±0.05) occurs via intersystem crossing (ISC) to the underlying singlet PES forming ¹HCCN(cyanomethylene)+CO. The O(¹D) reaction exhibits the same two channels, with the relative CO/H yield slightly larger. (ii) The O(³P)+CH₂CHCN reaction leads to two main product channels, among a variety of possible open channels: (a) CH₂CNH(ketenimine)+CO (dominant, BF=0.87±0.05), formed via efficient ISC, (b) HCOCHCN+H (BF=0.13±0.05), occurring adiabatically on the triplet PES. Both ketenimine and acrylonitrile have been detected toward the same star-forming regions (as in Sagittarius B2(N) hot core). Ketenimine is often neglected by astrophysical modelers, with respect to its more abundant CH₃CN isomer, and also the reaction O(³P)+acrylonitrile is overlooked in models. The O(¹D)+CH₂CHCN reaction mainly leads to formation of CH₂CNH+CO adiabatically on the singlet PES; these results can help improving models related to the chemistry of interstellar ice and cometary comas, where O(¹D) reactions are believed to play an important role. Overall, our results on the title reactions are expected to be useful for improving models of combustion and extraterrestrial environments.

¹ Casavecchia, P. *et al.* Probing the Dynamics of Polyatomic Multichannel Elementary Reactions by Crossed Molecular Beam Experiments with Soft Electron-Ionization Mass Spectrometric Detection. *PCCP* 11, 46-65, 2009.

² Casavecchia, P. *et al.* Reaction Dynamics of Oxygen Atoms with Unsaturated Hydrocarbons from Crossed Molecular Beam Studies: Primary Products, Branching Ratios and Role of Intersystem Crossing. *Int. Rev. Phys. Chem.* 34, 161-204, 2015.

³ Liang, P. *et al.* Reactions O(³P, ¹D) + HCCCN(X¹Σ⁺) (Cyanoacetylene): Crossed-Beam and Theoretical Studies and Implications for the Chemistry of Extraterrestrial Environments. *J. Phys. Chem. A* 127, 685-703, 2023.

⁴ Pannacci, G. *et al.* Combined crossed-beams and theoretical study of the O(³P,¹D) + acrylonitrile (CH₂CHCN) reactions and implications for combustion and extraterrestrial environments. Submitted to *PCCP*, 2023.

An Experimental and Theoretical Investigation of the $N(^2D) + \text{Benzene}$ Reaction with Implications for the Photochemical Models of Titan

Gianmarco Vanuzzo,^a Adriana Caracciolo,^a Dimitrios Skouteris,^b Marzio Rosi,^c Leonardo Pacifici,^a
Nadia Balucani,^a Kevin M. Hickson,^d Jean-Christophe Loison,^d Michel Dobrijevic^e
and Piergiorgio Casavecchia^a

^a *Dipartimento di Chimica, Biologia e Biotecnologie, Università degli Studi di Perugia, 06123 Perugia, Italy*

^b *Master-Tec SrL, 06128 Perugia, Italy*

^c *Dipartimento di Ingegneria Civile e Ambientale, Università degli Studi di Perugia, 06100, Perugia, Italy*

^d *Univ. Bordeaux, CNRS, Bordeaux INP, ISM, UMR 5255, F-33400 Talence, France*

^e *Univ. Bordeaux, CNRS, LAB, UMR 5804, F-33600 Pessac, France*

Email: piergiorgio.casavecchia@unipg.it

ABSTRACT

We report on a combined experimental and theoretical investigation of the $N(^2D) + C_6H_6$ (benzene) reaction of relevance in the atmospheric chemistry of Titan. Experimentally, the reaction was studied (i) under single-collision conditions by the crossed molecular beams (CMB) scattering method with mass spectrometric detection and time-of-flight analysis at the collision energy (E_c) of 31.8 kJ/mol to determine the primary products and their branching fractions (BFs),^{1,2,3} and (ii) in a continuous supersonic flow reactor to determine the rate constant as a function of temperature from 50 K to 296 K.⁴ Theoretically, electronic structure calculations of the doublet C_6H_6N potential energy surface (PES) were performed to assist the interpretation of the experimental results and characterize the overall reaction mechanism. The reaction is found to proceed via barrierless addition of $N(^2D)$ to the aromatic ring of C_6H_6 , followed by formation of several cyclic (five-, six-, and seven-membered ring) and linear isomeric C_6H_6N intermediates that can undergo unimolecular decomposition to bimolecular products. Statistical (RRKM/Master Equation) calculations of product BFs on the theoretical PES were carried out under the conditions of the CMB experiments and at the temperatures relevant for Titan's atmosphere. In all conditions the ring-contraction channel leading to C_5H_6 (cyclopentadiene) + CN is dominant, while minor contributions come from the channels leading to *o*- C_6H_5N (*o*-N-cycloheptatriene radical) + H, C_4H_4N (pyrrolyl) + C_2H_2 (acetylene), C_5H_5CN (cyano-cyclopentadiene) + H, and *p*- C_6H_5N + H.⁵ Rate constants (which are close to the gas kinetic limit at all temperatures, with the recommended value of $(21.9 \pm 3.0) \times 10^{-11} \text{ cm}^3 \text{ s}^{-1}$ over the 50-296 K range) and BFs have been used in a photochemical model of Titan's atmosphere to simulate the effect of the title reaction on the species abundances (including any new products formed) as a function of the altitude.⁵

¹ Casavecchia, P. *et al.* Probing the Dynamics of Polyatomic Multichannel Elementary Reactions by Crossed Molecular Beam Experiments with Soft Electron-Ionization Mass Spectrometric Detection. *PCCP* 11, 46-65, 2009.

² Casavecchia, P. *et al.* Reaction Dynamics of Oxygen Atoms with Unsaturated Hydrocarbons from Crossed Molecular Beam Studies: Primary Products, Branching Ratios and Role of Intersystem Crossing. *Int. Rev. Phys. Chem.* 34, 161-204, 2015.

³ Vanuzzo, G. *et al.* The $N(^2D) + CH_2CHCN$ (Vinyl Cyanide) Reaction: A Combined Crossed Molecular Beam and Theoretical Study and Implications for the Atmosphere of Titan. *J. Phys. Chem. A* 126, 6110-6123, 2022.

⁴ Hickson, K. M. *et al.* A kinetic study of the $N(^2D) + C_2H_4$ reaction at low temperature. *PCCP* 22, 14026-14035, 2020.

⁵ Balucani, N. *et al.* An experimental and theoretical investigation of the $N(^2D) + C_6H_6$ (benzene) reaction with implications for the photochemical models of Titan, *Faraday Discuss.*, in press (DOI: 10.1039/D3FD00057E), 2023.

Real-Space Laser-Induced Fluorescence Imaging of OH Inelastic Scattering at the Gas-Liquid Interface

Maksymilian J. Roman, Daniel R. Moon, Adam G. Knight, Paul D. Lane, Stuart J. Greaves,
Matthew L. Costen and Kenneth G. McKendrick

*Institute of Chemical Sciences, Heriot-Watt University, Edinburgh EH14 4AS, United Kingdom.
Email: m.l.costen@hw.ac.uk*

ABSTRACT

Gas-Liquid interfaces, and the heterogeneous processes that occur at them, have been the subject of much less experimental and theoretical study than the gas-phase or gas-solid interface. Relatively little is known about the structure of liquid surfaces, and the interplay between the surface structure and the elementary chemical processes resulting from gas-liquid interaction. In recent years, new experimental techniques and theoretical methodologies have begun to provide detailed understanding in this area. We have developed a gas-liquid scattering apparatus with planar laser-induced-fluorescence imaging of the real-space scattering distribution. Combined with a pulsed supersonic DC discharge source of OH, we have used this apparatus to study the dynamics of the inelastic collisions of OH radicals with the surfaces of the inert liquid perfluoropolyether (PFPE), and also the surfaces of the potentially reactive hydrocarbons squalane (saturated) and squalene (unsaturated).

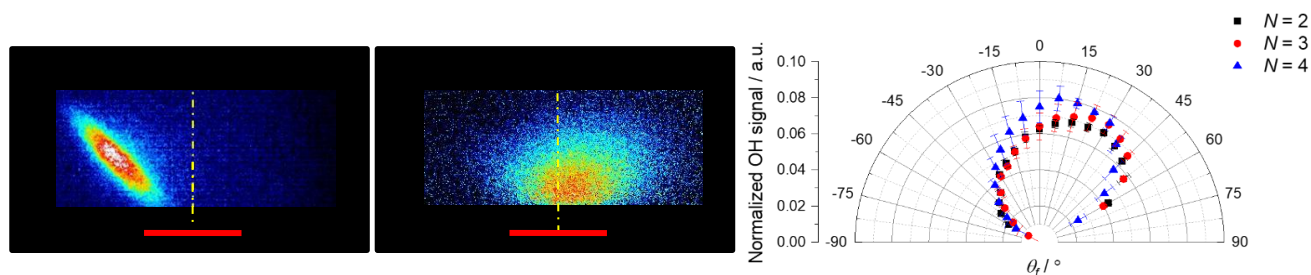


Figure 1. LIF image of incident 45° OH molecular beam (left), LIF image of OH inelastic scattering in $N' = 3$ from PFPE Surface (center), scattering angle distributions from PFPE as a function of N' (right). The red line indicates the position of the liquid surface, the yellow dashed line is the surface normal at the central impact location of the incident molecular beam.

Analysis of images taken in a time-series that spans before and after collision reveals that the OH radicals are scattered from all 3 liquids, and for both normal and 45° incident angles, with a predominately superthermal speed distribution, with no strong evidence for a substantial thermalized component. Angular scattering distributions are determined from both time-series and single-time images for each incident angle, each liquid and as a function of OH rotational state. Significant anisotropy is observed in the scattering for 45° incident angle, with the scattering angle distribution varying as a function of liquid and final N' . We discuss the observed differences in the scattering dynamics in the context of both the inelastic and reactive processes occurring at the surfaces of the three liquids.

Dynamics of Optically Centrifuged N₂O in Extreme Rotational States Studied with Transient IR Absorption Spectroscopy

Simone A. DeSouza, Michael E. Ritter, Christopher R. Lukowski, and Amy S. Mullin

Department of Chemistry and Biochemistry, University of Maryland, College Park
Email: sdesouz1@umd.edu

ABSTRACT

The behavior of molecules with large amounts of rotational energy is a largely unexplored area in physical science. Molecules in high energy rotational states are observed as products of reactions and collisional energy transfer, but they are not easily prepared by traditional experimental methods. High rotational states can be prepared using an optical centrifuge, which is an ultrafast laser-based method that selectively populates molecules with inverted rotational distributions. Investigating the behavior of molecules in extreme rotational states enhances our understanding of fundamental energy transfer processes, energy partitioning in vibration and rotation, and centrifugal distortion in molecules in extreme J states. In this project, an optical centrifuge is combined with a high-resolution transient IR absorption spectrometer to explore the dynamics of optically centrifuged N₂O (00⁰1-00⁰0) with J=100-200 and rotational energies up to 16,000 cm⁻¹.

A tunable optical centrifuge was used to selectively optimize N₂O population by controlling the bandwidth of the optical pulses. Figure 1a shows optical trap intensity profiles as a function of instantaneous angular frequency Ω_{OC} for the full bandwidth pulses and for pulses with reduced bandwidth to preferentially populate the J=140 and 160 rotational states. The nascent distributions of centrifuged molecules were measured with high-resolution transient IR absorption spectroscopy at $\lambda=4.4\ \mu\text{m}$ and a spectroscopic pressure of 2.5 Torr. The IR transitions used for this study were first identified using transient spectroscopy of optically centrifuged N₂O.^{1,2} Figures 1b and 1c show the inverted nascent rotational distributions for the two reduced-bandwidth traps at t=300 ns. Transient IR Doppler line profiles were measured to

characterize the translational energy transfer of optically centrifuged molecules and polarization-sensitive spectroscopy was used to investigate orientational anisotropy dynamics and relaxation kinetics of the optically centrifuged molecules. The orientational anisotropy of the centrifuged molecules increases as a function of J and lower J-states have higher translational energies as a result of impulsive collisions between centrifuged molecules and thermal bath molecules. The translational energies of lower J-states increase as a function of time as rotational energy is converted to translational energy through inelastic collisions. The time-dependence of the high-J tail populations shows that the collisional relaxation rate constants are approximately half that of the Leonard-Jones collisional rate constant. The results are compared with previous dynamics studies on optically centrifuged CO molecules.³ This project has been funded through the NSF.

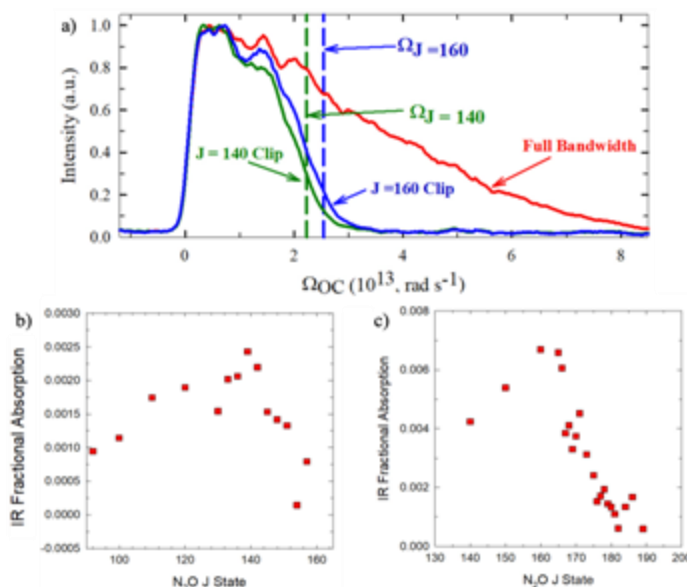


Figure 1. a) Profiles for the optical centrifuge traps used in this study. Nascent rotational distributions of N₂O optimized for b) J=140 and c) J=160.

¹ Yuan, L. Toro, C. *et al.* Spectroscopy of Molecules in very High Rotational States using an Optical Centrifuge. *Faraday Discussions* 150, 101-111, 2011.

² Ogden, H. *et al.* Transient IR (00⁰1-00⁰0) Absorption Spectroscopy of Optically Centrifuged N₂O with Extreme Rotation up to J=205. *JSQRT* 246, 106867, 2020.

³ Laskowski, M.R. *et al.* Rotational Energy Transfer Kinetics of Optically Centrifuged CO Molecules Investigated through Transient IR Spectroscopy and Master Equation Simulations. *Faraday Discussions* 238, 87-102, 2022.

CPUF in an Extended Laval Nozzle: Low Temperature Kinetics of the HCO + NO Reaction with Conditions Measured Using REMPI

Shameemah Thawoos,^a Matthew L. Edlin,^a Ranil M. Gurusinghe,^b Nicolas Suas-David^c
and Arthur G. Suits^a

^a Department of Chemistry, University of Missouri, Columbia, MO, 65211 USA.

Email: mle367@umsystem.edu

^b Department of Chemistry, Tennessee Technical University, Cookeville, TN 38505 USA

^c Univ Rennes, CNRS, Institut de Physique de Rennes - UMR 6251, F-35000 Rennes, France

ABSTRACT

In the CRESU technique,¹ pioneered in Rennes, a uniform supersonic flow serves as a wall-less reactor for low temperature kinetics measurements. The traditional method of detection employed with CRESU is laser induced fluorescence (LIF). One of the major drawbacks of LIF is the limited number of species that can be probed, and this range can be greatly expanded by using chirped-pulse rotational spectroscopy, an approach we term CPUF for chirped-pulse/uniform flow.^{2,3} Detection by CPUF requires monitoring the free induction decay of the species. However, the high collision frequency in high-density uniform supersonic flows can interfere with the free induction decay and attenuate the signal. One way to overcome this is to use sampling methods, such as airfoil or skimmer sampling. However, this requires complicated experimental designs with differential pumping systems and can have interference from shocks in the sampling region and thus may not be ideal for studying reaction kinetics. This has led us to develop an extended Laval nozzle which creates a uniform flow within the nozzle itself, after which the gas undergoes a *shock-free secondary expansion* to a cold, low pressure condition ideal for CP-FTMW detection. However, impact pressure measurements, commonly used to characterize Laval flows, cannot be used to monitor the flow within the nozzle. Hence, we have implemented a REMPI (resonance-enhanced multiphoton ionization) detection scheme which allows interrogation of the conditions of the flow directly inside the extended nozzle, confirming fluid dynamics simulations of the flow environment. We have built an extended nozzle designed for a 20 K He flow and characterized the flow within the nozzle using (1+1) REMPI of a very dilute sample of NO. We will describe the development of the new extended flow along with its characterization using REMPI and application to studies of the low temperature reaction kinetics of HCO with NO as co-reactant. The data gathered in this study demonstrates the potential of both the REMPI and CPUF methods for low temperature kinetics.

¹ I. R. Sims; J.-L. Queffelec; A. Defrance; C. Rebrion-Rowe; D. Travers; P. Bocherel; B. R. Rowe; I. W. M. Smith. "Ultralow temperature kinetics of neutral-neutral reactions. The technique and results for the reactions CN+O₂ down to 13 K and CN+NH₃ down to 25 K". *J. Chem. Phys.* 100, 4229–4241 (1994)

² James M. Oldham; Chamara Abeysekera; Baptiste Joalland; Lindsay N. Zack; Kirill Prozument; Ian R. Sims; G. Barratt Park; Robert W. Field; Arthur G. Suits. "A chirped-pulse Fourier-transform microwave/pulsed uniform flow spectrometer. I. The low-temperature flow system". *J. Chem. Phys.* 141, 154202 (2014)

³ Chamara Abeysekera; Lindsay N. Zack; G. Barratt Park; Baptiste Joalland; James M. Oldham; Kirill Prozument; Nuwandi M. Ariyasingha; Ian R. Sims; Robert W. Field; Arthur G. Suits. "A chirped-pulse Fourier-transform microwave/pulsed uniform flow spectrometer. II. Performance and applications for reaction dynamics". *J. Chem. Phys.* 141, 214203 (2014)

The Collisional 2:1 Rotation-Vibration Quasiresonance

Jacob Fanthorpe,^a Simon Rothman,^b and Brian Stewart

Department of Physics, Wesleyan University, Middletown, CT, USA. Email: bstewart@wesleyan.edu

^aAb Initio Software, Lexington, MA, USA

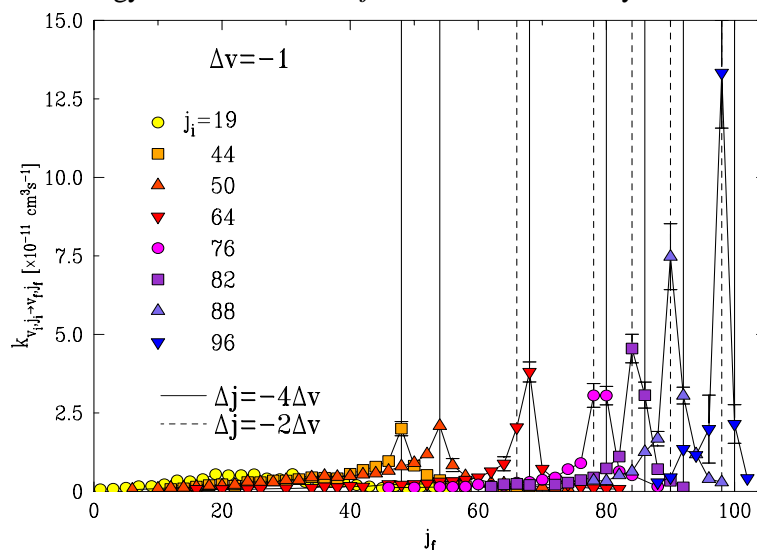
^bDepartment of Physics, Massachusetts Institute of Technology, Cambridge, MA, USA

ABSTRACT

At low rotational angular momentum j , atom-diatom collisions at thermal energies are typically rotationally sudden but vibrationally adiabatic, resulting in large rotationally inelastic and small vibrationally inelastic rate constants. In contrast, at elevated j , the molecular rotational frequency can be a small-integer submultiple of the vibrational frequency. At such resonances, collisional energy transfer between rotation and vibration becomes extremely facile, leading to dramatically increased level-to-level vibrationally inelastic rate constants. The resonance condition also leads to sharply-peaked rotational distributions governed by the rule $\Delta j^{peak} = -n\Delta v$, where v denotes the vibrational action or quantum number and n is the order of the resonance.

The 4:1 resonance in Li_2 ($1A^1\Sigma_u^+$) has been studied experimentally at $j=64$ in previous work.¹ The 4:1 rule persists well away from resonance, leading to the term *quasiresonance* to describe the phenomenon, in which the adiabatic invariants j and v are transiently replaced by a linear combination. In experiments and calculations, quasiresonance dominates rovibrationally inelastic energy transfer between $j=42$ and 76 in this system.¹ The dynamical origin of quasiresonance has been explored by Ruiz and Heller.²

Using the same laser-induced fluorescence technique as in previous studies, we have extended measurements to initial values of j as high as 96 and final values up to 112. Making these measurements necessitated increasing the range of spectroscopic measurements of the Li_2 A-X system. We determined the frequencies of 4818 previously unmeasured transitions, up to the X-state predissociation limit for some v'' values. These results made possible the first observation of a quasiresonant



transition, between the 4:1 and 2:1 quasiresonant regions in Li_2 -X, with $X=\text{Li}$ and Xe . While the 2:1 resonance itself remains beyond the reach of the experiments, the 2:1 quasiresonant rule $\Delta j^{peak} = -2\Delta v$ is very clearly dominant at the highest values of j . The very strong peaking and large rate constants previously observed near $j=64$ are further enhanced. The figure shows rate constants for $\Delta v = -1$ in the Li_2 -Li system.

At some initial values of j , both the 2:1 and 4:1 quasiresonances are observable in a single rate constant distribution. We have explored the classical origins of this behavior and found that the two resonant peaks arise from different classes of collisions with rotational and orbital angular momentum either aligned or anti-aligned. While classical mechanics seems to capture the essence of the dynamics, quantitative comparison is made challenging by the shortcomings of available binning methods in the presence of sharp resonance features.

¹ Stewart, B., Magill, P. D. and Pritchard, D. E., Quasi-resonant Vibration-Rotation Transfer in Inelastic Li_2^*-Ne Collisions. *JPCA* **104**, 10565-10575, 2000.

² Ruiz, A. and Heller, E. J., Quasiresonance: Switching Internal Energy Transfer On and Off. *JPCA* **109**, 11578-11586, 2005.

Toward Understanding Dynamics of Associative Ionization in Hypersonic Flows

Casey D. Foley and Arthur G. Suits

Department of Chemistry, University of Missouri, 601 S College Ave, Columbia, MO 65211, USA

Email: cdfoley@mail.missouri.edu

ABSTRACT

Rapid variation of flow thermodynamics in shocks during hypersonic flight leads to dissociation of O_2 and N_2 to atomic constituents and ablate surfaces that are encountered to produce carbon atoms. Associative ionization of C, N, and O atoms, primarily $N + O \rightarrow NO^+ + e^-$, form a plasma that can interfere with radio communication and compromise the performance of onboard sensors. Complex chemistry due to rapidly varying nonequilibrium flow conditions in hypersonic systems has been modeled, but suitable experimental data is lacking. Only a single direct measurement of associative ionization under conditions relevant to hypersonic flows has been made.¹ Dissociative recombination measurements have indirectly obtained associative ionization cross sections for NO^+ , CO^+ , and O_2^+ assuming detailed balance.² However, only ground state ions were used in these dissociative recombination studies, despite evidence of branching to vibrationally excited ions by Ringer and Gentry.

Modifications to a crossed molecular beam apparatus are being made to allow for fast atom beam production to study associative ionization processes. A well-defined fast atom beam is crucial for understanding associative ionization dynamics and must be versatile, tunable, and has a narrow kinetic energy spread. Here, atomic ion beams are produced via a pulsed discharge from a Trickle valve. High velocity atom beams are then produced via charge exchange of atomic ions with various gases. Furthermore, implementation of 3D electron-ion coincidence detection by velocity map imaging will allow for identification of contributing electronic states and determination of the vibrational distribution of the product ions.³ We will measure the associative ionization excitation functions and electronic state dependence for C, N and O atoms. The internal state distribution of the product ions provide a key test of the theoretical description of the process. The results will then be available for use in multiscale computer modeling of plasma formation in hypersonics.

¹ Ringer, G. and Gentry W.R. A merged molecular beam study of the endoergic associative ionization reaction $N(^2D) + O(^3P) \rightarrow NO^+ + e^-$. *J. Chem. Phys.* 71, 1902–1909, 1979.

² Le Padellec, A. Partial Near Threshold Cross Sections for the Associative Ionization to Form CO^+ , NO^+ and O^+ . *Physica Scripta*. 71, 621–626, 2005.

³ Basnayake, G., Ranathunga, Y., Lee, S.K., and Li, W. Three-dimensional (3D) velocity map imaging: from technique to application. *J. Phys. B: At. Mol. Phys.*, 55, 023001, 2022.

Steric effects in rotationally inelastic collisions: Imaging k - j - k' correlations in NO(A) + Ne scattering.

M. Fournier, Kenneth G. McKendrick and Matthew L. Costen

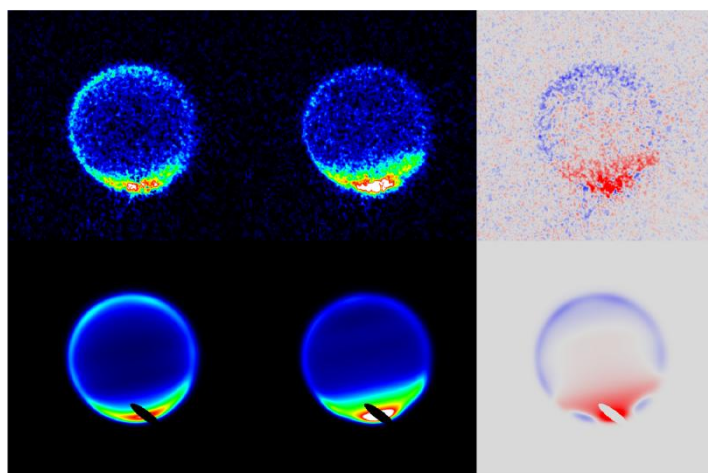
Institute of Chemical Sciences, Heriot-Watt University, Edinburgh, U.K.

Email: m.fournier@hw.ac.uk

ABSTRACT

We report what we believe to be the first ever experimental measurement of state-to-state k - j - k' correlations in rotationally inelastic scattering.

We have used crossed-molecular beam scattering with velocity-map imaging, combined with optical state-selection, to study the stereodynamics of rotational energy transfer of electronically excited NO($A^2\Sigma^+$, $v = 0$, $N = 4$, $j = 3.5$) in collisions with Ne. A linearly polarized laser prepares this initial state with a rotational alignment, j , that is preferentially either perpendicular to the pre-collision velocity vector, k , or near parallel to k . The products of rotationally inelastic scattering, NO($A^2\Sigma^+$, $v = 0$, $N' = 0, 1, 3, 5, 9, 10$), are probed by 1+1' REMPI. The saturated probe step is essentially insensitive to product rotational alignment, j' , resulting in velocity-map images that contain k - j - k' correlations. Analysis of the images provides the conventional differential cross sections, and two polarization-resolved differential cross sections, which describe the dependence of the observed scattering on the initial j alignment as a function of scattering angle. Strong k - j - k' correlations, that vary systematically with final state N' and with $\Delta N'$ negative or positive are observed. The results are consistent with theoretical predictions from quantum scattering calculations performed on a literature ab initio potential energy surface. Representing the results as the respective differential cross sections for limiting 'propellor', 'cartwheel' and 'frisbee' alignments of j provides physical insight into the observed scattering dynamics.



Velocity mapped images for $N'=0$ NO(A)-Ne scattering. Images left to right are Horizontal, Vertical, V-H (red = high). Top is data, bottom is fit to QS calculations.

Theoretical investigation of the reactions of OH with ethane and glycine

B. Gruber, V. Tajti and G. Czakó

MTA-SZTE Lendület Computational Reaction Dynamics Research Group, Interdisciplinary Excellence Centre and Department of Physical Chemistry and Materials Science, University of Szeged, Szeged, Hungary. Email: gbalazs96@gmail.com

ABSTRACT

We perform a high-level study of the dynamics of the OH + ethane reaction.¹ In the first place, we optimized the geometries of the stationary points of the reaction with the CCSD(T)-F12b method using aug-cc-pVTZ basis set. Three reaction paths are taken into account: hydrogen-abstraction, hydrogen-substitution and methyl-substitution. In the case of substitution two different mechanisms are considered: Walden inversion and front-side attack. In order to further advance the punctuality, we carry out single-point energy calculations at the level of CCSD(T)-F12b/aug-cc-pVQZ utilizing the above-determined structures. Furthermore, five different energy corrections are taken into consideration to go below the sub-chemical accuracy: the effect of the core electrons, δT , $\delta(Q)$, the scalar relativistic and the spin-orbit contributions. After the characterization of the stationary points of the OH + ethane reaction, we aim to develop an analytical *ab initio* full-dimensional potential energy surface (PES) to study the dynamics in detail.² The PES development is carried out at the level of a composite method (CCSD(T)-F12b/aug-cc-pVDZ + (MP2-F12/aug-cc-pVTZ – MP2-F12/aug-cc-pVDZ) using the ROBOSURFER program package. All in all, 85 000 quasi-classical trajectories are run and we determine the following quantities: classical and adiabatic energies of the stationary points, reaction probability values, integral cross sections, scattering angle distributions, attack angle distributions of the reactants, translational, rotational, vibrational and internal energy distributions, and rotational quantum number distributions. As a next step, we investigate the dynamics utilizing the current PES by exciting several normal-modes (one for OH and five for ethane). Quasi-classical simulations are carried out and we compute the same quantities as before. Furthermore, we also calculate the mode-specific vibrational state distributions in case of the H₂O product molecule.

We also study the OH + glycine reaction being interested in only the hydrogen-abstraction pathways.³ The abstraction can happen from three different groups of the glycine molecule: NH₂, CH₂ and COOH. The reactants and products and their conformers were already revealed previously. We determine the most possible conformer-structures of the transition states and post-reaction minima at the level of CCSD(T)-F12b/aug-cc-pVDZ. Higher level energy calculations are carried out with the CCSD(T)-F12b method using two different basis sets, aug-cc-pVTZ and aug-cc-pVQZ. The previously-mentioned energy corrections are also calculated. All in all, we successfully identify 5 transition states and 2 post-reaction minima in the case of the CH₂ group, 5 transition states and 19 post-reaction minima considering the NH₂ pathway, as well as 5 transition states in the COOH region. Utilizing these structures an analytical *ab initio* full-dimensional PES development is performed using a ManyHF-based coupled-cluster-quality composite method.

¹ B. Gruber and G. Czakó. Benchmark *ab initio* characterization of the abstraction and substitution pathways of the OH + CH₄/C₂H₆ reactions. *Phys. Chem. Chem. Phys.* 22, 14560, 2020.

² B. Gruber, V. Tajti and G. Czakó. Full-dimensional automated potential energy surface development and dynamics for the OH + C₂H₆ reaction. *J. Chem. Phys.* 157, 074307, 2022.

³ B. Gruber and G. Czakó. High-level *ab initio* mapping of the multiple H-abstraction pathways of the OH + glycine reaction. *Phys. Chem. Chem. Phys.* 25, 5271, 2023.

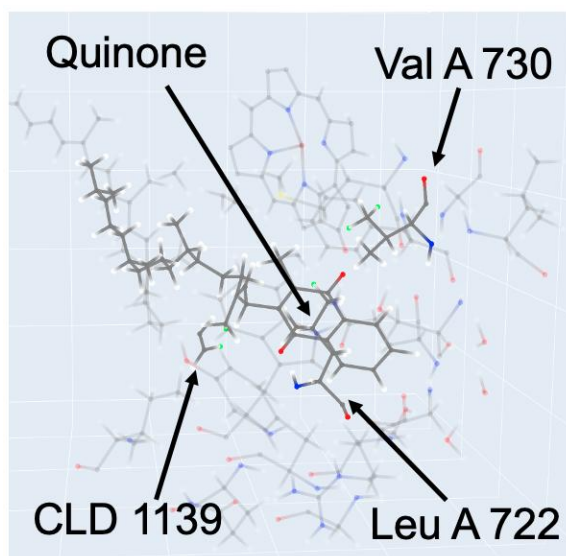
Electron Spin Coherences in Photosystem I

Yeonjun Jeong, Ahren W. Jasper, Jasleen K. Bindra, Jens Niklas, and Oleg Poluektov

Chemical Sciences and Engineering Division, Argonne National Laboratory, Argonne, IL 60439, USA. Email: yeonjun.jeong@anl.gov

ABSTRACT

Microsecond coherence times are observed in the $P^+A_1^-$ entangled electron spin pair created upon excitation of photosystem I in cyanobacteria.¹ Important environmental features in the spin pair's decoherence, such as protein residues and the distance of the bath spins from the central spins, are identified using spin dynamics calculations under the cluster-correlation expansion (CCE) approximation²⁻⁴. Notably, the protons within the distance range of 5-8Å are found to be the dominant contributors. In a more microscopic picture, important two-spin decoherence drivers, as well as individual nuclear spins, are characterized by controlling the spin-spin couplings in the system's interaction Hamiltonian.



¹Canfield, P. et al. Density-Functional Geometry Optimization of the 150 000-Atom Photosystem-I Trimer. *J. Chem. Phys.* 124, 024301, 2006.

²Yang, W. and Liu, R.-B. Quantum Many-Body Theory of Qubit Decoherence in a Finite-Size Spin Bath. *Phys. Rev. B* 78, 085315, 2008.

³Yang, W. and Liu, R.-B. Quantum Many-Body Theory of Qubit Decoherence in a Finite-Size Spin Bath. II. Ensemble Dynamics. *Phys. Rev. B* 79, 115320, 2009.

⁴Onizhuk, M. and Galli, G. PyCCE: A Python Package for Cluster Correlation Expansion Simulations of Spin Qubit Dynamics. *Adv. Theory Simul.* 4, 2100254, 2021.

Intermolecular Interactions Drive Chemical Outcomes: Infrared Activation of Open-Shell Collision Complexes

John P. Davis, Ruby W. Neisser and Nathanael M. Kidwell

William & Mary, Williamsburg, VA 23187-8795, USA. Email: nmkidwell@wm.edu

The accurate prediction of bimolecular collision outcomes is crucial for understanding chemical transformations on multidimensional potential energy surfaces. A comprehensive understanding of the reactive and nonreactive pathways demands that all factors affecting the collision be characterized to accelerate the predictive modeling of chemical reactivity. To this end, the bimolecular collision outcomes can be systematically explored by preparing reactants in the entrance channel prior to reaction. Experimental studies in this laboratory have utilized infrared action spectroscopy and velocity map imaging of products to probe the structure, vibrational frequencies, and nonreactive energy-exchange mechanisms of open-shell collision complexes between nitric oxide (NO) and alkane partners (CH_4 and C_2H_6). As shown in Figure 1, the isomer-specific infrared spectroscopy of NO- CH_4 and NO- C_2H_6 complexes in the CH stretch region reveals the intermolecular interactions between the collision partners. Furthermore, the spectra indicate that ultrafast vibrational predissociation takes place when the asymmetric CH stretch is activated, signifying that this vibrational mode couples more directly with the intermolecular reaction coordinate. The figure also illustrates that the ion image anisotropy is largely determined by the probed rotational quantum number of NO (J'') products. For a subset of NO (J'') fragments, the ion images and total kinetic energy release distributions show an anisotropic component at low relative translation ($\sim 225 \text{ cm}^{-1}$) indicating a prompt dissociation mechanism. However, for other detected NO (J'') products, the ion images and total kinetic energy release distributions are bimodal, in which the anisotropic component is accompanied by an isotropic feature at high relative translation ($\sim 1400 \text{ cm}^{-1}$) signifying a slow dissociation pathway. The mechanistic pathways prior to and following infrared activation of NO- CH_4 and NO- C_2H_6 complexes will be presented to assess the bimolecular collision impacts in the atmosphere and non-thermal environments.

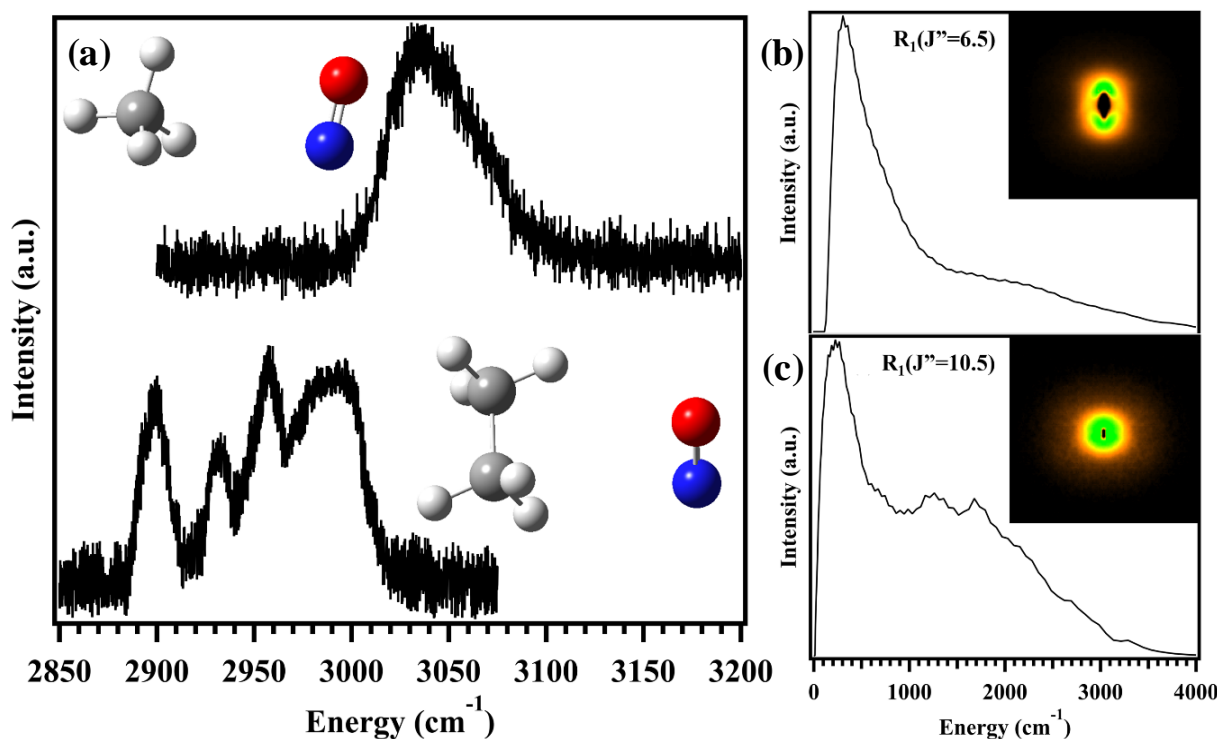


Figure 1: (a) Infrared action spectra of (top) NO- CH_4 and (bottom) NO- C_2H_6 collision complexes. (b, c) Velocity map ion images and total kinetic energy release distributions of NO ($X^2\Pi$, $v''=0$, J'' , F_n , Λ) + CH_4 products from infrared activation of NO- CH_4 complexes.

Sulfur (3P) reaction with conjugated dienes forms thiophenes under single collision conditions

Jinxin Lang,^a Hongwei Li,^{a,b} Casey D. Foley,^a Shameemah Thawoos,^a Matthew Edlin,^a
Judit Zador^c and Arthur G. Suits^a

^aDepartment of Chemistry, University of Missouri, Columbia, MO 65211. Email: jinxinlang@mail.missouri.edu

^bState Key Laboratory of Molecular Reaction Dynamics and Dalian Coherent Light Source, Dalian Institute of Chemical Physics, Chinese Academy of Sciences, Dalian 116023, China

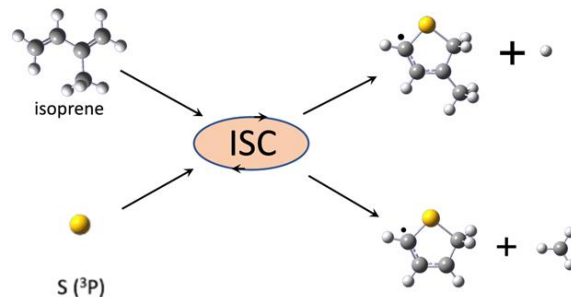
^cCombustion Research Facility, Sandia National Laboratories, Livermore, California 94551

ABSTRACT

Sulfur's abundance and presence in organic molecules, notably thiophenes, make it a vital element in understanding the origin and evolution of life and the chemistry of the universe. While detailed dynamics studies on $S(^3P)$ are lacking, Gunning and Strausz conducted studies exploring the kinetics and product branching.¹ A highly stereospecific addition of $S(^3P)$ across a double bond was observed, resembling the behavior of $S(^1D)$ and singlet species in general. They attributed this stereospecificity to asymmetric addition, forming a long-lived triplet biradical followed by

rapid intersystem crossing (ISC). Here, we utilized crossed-beam velocity map imaging and high-level ab initio/transition state theory modeling to investigate the reaction of $S(^3P)$ with 1,3-butadiene and isoprene under single collision conditions.² Coupled cluster calculations using KinBot³ indicate intersystem crossing to the singlet surface, leading to the formation of various long-lived intermediates, including 5-membered heterocycles. In

the case of the butadiene reaction, our experimental observations revealed the detected 2H-thiophenyl radical through H loss and confirmed the predicted formation of thiophene through H_2 loss and thioketene through ethene loss. Complementary chirped pulse microwave measurements in a uniform flow reinforced the formation of thioketene. For the isoprene reaction, we experimentally observed analogous products, but also the methyl loss (C_4H_5S) radical. Theoretical calculations suggest a range of reaction products analogous to reaction of $S(^3P)$ with butadiene. Interestingly, the results obtained for $S(^3P) + 1,3$ -butadiene highlight a direct cyclization pathway to the aromatic product, contrasting significantly with the behavior observed in the analogous $O(^3P)$ reaction. The different behavior is primarily attributed to the substantial differences in C-O and C-S bond energies among the potential products.



¹ Sidhu, K.; Lown, E.; Strausz, O.; Gunning, H. The reactions of sulfur atoms. VI. The addition to C4 olefins. A stereospecific triplet-state reaction. *J. Am. Chem. Soc.*, 88, 254–263, 1966.

² Li, H. and Suits, A.G. Universal crossed beam imaging studies of polyatomic reaction dynamics. *Phys. Chem. Chem. Phys.*, 22, 11126, 2020.

³ Van de Vijver, R. and Zádor, J. KinBot: Automated stationary point search on potential energy surfaces. *Comp. Phys. Comm.*, 248, 106947, 2020.

The Role of the Pre-reaction Complex in the Dynamics of the $\text{CH}_3 + \text{HBr} \rightarrow \text{CH}_4 + \text{Br}$ Reaction

Péter Szabó^a and György Lendvay^b

^aDepartment of Chemistry, KU Leuven, Celestijnenlaan, 200F 3001 Leuven, Belgium

^bInstitute of Materials and Environmental Chemistry, Research Centre for Natural Sciences, Magyar tudósok krt. 2, 1117 Budapest, Hungary. Email: lendvay.gyorgy@ttk.mta.hu

ABSTRACT

The potential surface of the exothermic hydrogen abstraction reaction by CH_3 radicals from HBr involves a weakly bound hydrogen-bonded complex separated from the products by a submerged barrier. This kind of reaction is generally handled by statistical rate theories, although the energy redistribution in the weakly bound van der Waals complex is probably not fast. We studied the reaction using the quasiclassical trajectory (QCT) method to explore the correlation between reaction dynamics and the potential energy surface. The adequacy of the QCT method for this system was validated¹ by the good agreement of the excitation functions with those derived from reduced dimensionality quantum scattering calculations.

To understand the microscopic mechanism of the reaction, for each collision, the complex lifetime was calculated as the delay induced by the interaction with respect to free flight (which can be negative when the reactants attract each other).¹ The lifetime distribution for nonreactive collisions is structured and depends on the collision energy. The peaks of the distribution were assigned by analysis of the correlations between the impact parameter, the minimum reactant separation and the lowest energy accessed by the reacting system, recorded for each collision. In addition to reactive collisions, three classes of inelastic collisions were identified: quasi-elastic, trapped in the van der Waals well and frustrated reaction. Quasi-elastic collisions are fast and sample the repulsive wall of the potential energy surface. Among trajectories entering the potential well (forming a complex), the minority at low and the majority at high temperature leave the van der Waals well without reaction. The majority of the remaining “complex-forming” collisions lead to reaction, in the minority, called “frustrated reaction” the system visits regions of configuration space with potential energy below the bottom of the potential well, which is possible only on the product side of the barrier to reaction, temporarily forming a C-H bond and breaking the H-Br bond, but gets reflected from the repulsive C-H potential.

The vibrational energy of the breaking HBr bond speeds up the reaction at any collision energy.² Although the barrier is early, an extra attraction arises when the H-Br vibration is close to the outer turning point, because the bond is “half broken”. The H-Br amplitude is so large even in the vibrational ground state that the reaction is much faster than without the extra attraction, which is an interesting quantum effect. The reaction can be frozen by artificially reducing the H-Br amplitude.

The thermal rate coefficients obtained by trajectory calculations perfectly match the recent experiments, according to which the activation energy is negative at low temperatures, but switches to positive above about 600 K. The calculated excitation functions reveal that the negative activation energy, as expected, is induced by the attraction between the reactants: the reaction cross sections diverge when the collision energy is reduced towards zero. The large change of the activation energy can be reconciled with the existing thermochemical data only if one assumes that the activation energy of the reverse reaction also increases with the temperature.

¹ Galu, D., Xin, X., Wang, D., Szabó, P. and Lendvay, G. Theoretical dynamics studies of the $\text{CH}_3 + \text{HBr} \rightarrow \text{CH}_4 + \text{Br}$ reaction: integral cross sections, rate constants and microscopic mechanism. *Phys. Chem. Chem. Phys.* 24, 10548–10560, 2022.

² Csorba, B., Szabó, P., Góger, S. and Lendvay, G. The Role of Zero-Point Vibration and Reactant Attraction in Exothermic Bimolecular Reactions with Submerged Potential Barriers: Theoretical Studies of the $\text{R} + \text{HBr} \rightarrow \text{RH} + \text{Br}$ ($\text{R} = \text{CH}_3, \text{HO}$) Systems, *J. Phys. Chem. A* 125, 8386–8396, 2021.

OH Roaming in the Unimolecular Decay of the Alkyl Substituted Criegee Intermediates

Tianlin Liu,^a Sarah N. Elliott,^b Meijun Zou,^a Michael F. Vansco,^b Christopher A. Sojdak,^a Charles R. Markus,^{c,d} Raybel Almeida,^e Kendrew Au,^e Leonid Sheps,^e David L. Osborn,^{e,f} Carl J. Percival,^c Craig A. Taatjes,^e Rebecca L. Caravan,^b Stephen J. Klippenstein^b and Marsha I. Lester^a

^a *Department of Chemistry, University of Pennsylvania, Philadelphia, Pennsylvania 19104-6323, USA.
Email: liutl@sas.upenn.edu*

^b *Chemical Sciences and Engineering Division, Argonne National Laboratory, Lemont, IL 60439, USA*

^c *NASA Jet Propulsion Laboratory, California Institute of Technology, Pasadena, CA 91109, USA*

^d *Division of Chemistry and Chemical Engineering, California Institute of Technology, Pasadena, CA 91125, USA*

^e *Combustion Research Facility, Mailstop 9055, Sandia National Laboratories, Livermore, CA 94551, USA*

^f *Department of Chemical Engineering, University of California, Davis, CA 95616, USA*

ABSTRACT

Alkene ozonolysis generates short-lived Criegee intermediates ($R_1R_2C=O^+-O^-$), which are a significant source of hydroxyl (OH) radicals in the atmosphere. While unimolecular decay of Criegee intermediates to OH products can occur promptly or following thermalization, recent experimental and theoretical studies suggest that an alternative roaming pathway leading to hydroxycarbonyl products may also occur. Experiments under thermalized conditions utilizing multiplexed photoionization mass spectrometry with tunable vacuum ultraviolet radiation have identified hydroxybutanone as a stable product arising from OH roaming in the unimolecular decay of the methyl-ethyl substituted Criegee intermediate $[(CH_3)(CH_3CH_2)COO, MECI]$. Hydroxybutanone is distinguished from isomeric MECI (m/z 88) by its distinctive photoionization threshold and a kinetic appearance profile that matches that for unimolecular decay of MECI. A comprehensive theoretical kinetic analysis has been conducted to characterize the OH roaming pathway for unimolecular decay of MECI, and evaluate rate constants and branching yields under laboratory and atmospheric conditions. Additional experiments generating CH_3CHOO , $(CH_3)_2COO$, and MECI in a capillary reactor tube followed by jet-cooling detect hydroxymethyl (CH_2OH) radicals utilizing 2+1 resonance-enhanced multiphoton ionization. The CH_2OH radical is a characteristic C-C fission product of hydroxycarbonyls due to insufficient collisional stabilization. The formation of hydroxycarbonyl and C-C fission products is expected to be a general result of roaming, which can reduce the yield of OH radicals produced from alkene ozonolysis.

Research at the University of Pennsylvania is supported by the National Science Foundation under grant CHE-1955068 and the US Department of Energy–Basic Energy Sciences under grant DEFG02-87ER13792. Argonne National Laboratory is supported by the USDOE, Office of Science, BES, Division of Chemical Sciences, Geosciences, and Biosciences under Contract No. DE-AC02-06CH11357. Sandia National Laboratories is a multimission laboratory managed and operated by National Technology and Engineering Solutions of Sandia, LLC, a wholly owned subsidiary of Honeywell International, Inc., for the USDOE's National Nuclear Security Administration under contract DE-NA0003525. The describes objective technical results and analysis. Any subjective views or opinions that might be expressed in the paper do not necessarily represent the views of the USDOE or the US Government. © 2022, California Institute of Technology.

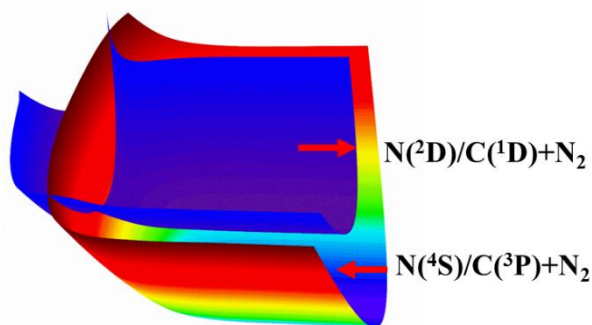
Quantum and Semiclassical Studies of Nonadiabatic Electronic Transitions of $C(^3P)/C(^1D)$ and $N(^4S)/N(^2D)$ via Collisions with N_2

Dandan Lu and Hua Guo

Department of Chemistry and Chemical Biology, University of New Mexico, Albuquerque, New Mexico 87131, USA. Email: ddlu@unm.edu

ABSTRACT

It is well established that electronically excited atomic species are much more reactive than their ground state counterparts. In the high-temperature boundary layer of a (re-)entry vehicle, atomic excitation could be facilitated by hyperthermal collisions with atmospheric molecules such as N_2 . The dynamics and kinetics of the nonadiabatic excitation of $C(^3P)$ to $C(^1D)$ and of $N(^4S)$ to $N(^2D)$ induced by hyperthermal collisions with N_2 molecules are investigated on coupled *ab initio* potential energy surfaces (PESs). These nonadiabatic spin-forbidden processes are modelled using both a quantum wave packet (WP) method and the semi-classical coherent switches with decay of mixing (CSDM) method. The multi-state quantum scattering calculations at selected partial waves found small transition probabilities, due to the weak spin-orbit coupling. Strong oscillations are also found in the probabilities for these two excitation processes, which are attributable to resonances supported by deep wells on PESs. The semi-classical method semi-quantitatively reproduces the quantum results when the zero-point energy of the product is properly taken into consideration. The calculated hyperthermal rate coefficients are expected to help constrain kinetic models for hypersonic simulations.



¹ Dandan Lu, Hua Guo. Quantum and Semiclassical Dynamics of Nonadiabatic Electronic Excitation of $C(^3P)$ to $C(^1D)$ by Hyperthermal Collisions with N_2 . *J. Phys. Chem. A*, 2023.

² Dandan Lu, Breno R. L. Galvão, Antonio J. C. Varandas, Hua Guo. Quantum and Semiclassical Studies of Nonadiabatic Electronic Transitions between $N(^4S)$ and $N(^2D)$ by Collisions with N_2 . Submitted to *Phys. Chem. Chem. Phys.*, 2023.

Collisional broadening of overtone lines in CO: measurements and calculations

Stephanie Schaertel and George C. McBane

Department of Chemistry, Grand Valley State University, Allendale, MI 49401, USA

Email: mcbaneg@gvsu.edu

ABSTRACT

Pressure broadening measurements in the 3-0 vibrational overtone band of CO are reported with neon and nitrogen as colliders. The Ne measurements, spanning the CO initial state range from $j=2$ to $j=20$, are compared with computed values based on the XC(fit) potential energy surface¹ of Dham et al. The computed values match well with the experimental results. The nitrogen measurements are compared with published experimental results² from other authors that were later retracted³ on the basis of concerns that the data analysis may have been in error. We find no evidence of errors in the earlier work.

¹ Ashok K. Dham, Frederick R.W. McCourt, and William J. Meath. An exchange-Coulomb model potential energy surface for the Ne-CO interaction. I. Calculation of Ne-CO van der Waals spectra. *J. Chem. Phys.* 130, 244310, 2009.

² A. Predoi-Cross, C. Hnatovsky, K. Strong, J.R. Drummond, and D. Chris Benner. Temperature dependence of self- and N₂-broadening and pressure-induced shifts in the 3 \leftarrow 0 band of CO. *J. Mol. Struct.* 695–696, 269, 2004.

³ A. Predoi-Cross, C. Hnatovsky, K. Strong, J.R. Drummond, and D. Chris Benner. Corrigendum to "Temperature dependence of self- and N₂-broadening and pressure-induced shifts in the 3 \leftarrow 0 band of CO" [*J. Mol. Struct.* 695–696 (2004) 269–286]. *J. Mol. Struct.* 1098, 4416, 2015.

Studying rotational-state and conformational effects in chemi-ionisation reactions

Amit Mishra,^a Ludger Ploenes,^a Patrik Stranak,^a Chao He,^a Sang K. Kim^b and Stefan Willitsch^a

^a Department of Chemistry, *University of Basel, Klingelbergstrasse 80*

Email: amit.mishra@unibas.ch

^b *Department of Chemistry, Daejeon 34141, Republic of Korea*

ABSTRACT

Conformers are the dominant isomers of complex molecules. The conformation of a molecule can have pronounced effects on its chemical reactivity. However, because they often interconvert into one another under ambient conditions, individual molecular conformations are difficult to isolate. Consequently, only sparse experimental data exists on the chemical properties of distinct conformers.¹ Over the past years, we have developed experimental methods to study conformational effects in ion-molecule reactions under single-collision conditions.^{2,3} We have recently built a new crossed-molecular-beam setup to extend our methodology to neutral-neutral reactions.⁴ This setup is equipped with an electrostatic deflector which enables the spatial separation of different conformers or individual rotational states of molecules based on their effective dipole moments.

As the first application of this new method, rotational-state-dependent chemi-ionisation reactions of carbonyl sulfide (OCS) with metastable neon atoms were investigated. A pronounced state-specific effect on the product branching ratio was observed. Our result suggests that OCS molecules in the rotational ground state $j = 0$ are a factor of 2.5 more reactive for dissociative ionisation than Penning ionisation compared to the $j = 1$ state.^{4,5} Moreover, for heavier molecules, the disentanglement of conformational and rotational-state effects can be difficult to analyse due to the involvement of several rotational states.⁵ Choosing conformers that can be chemically separated and have high interconversion barriers could disentangle the conformational and rotational state dependencies. Therefore, we chose to study the chemi-ionisation reaction of 1,2-dibromoethylene (DBE), the conformers of which can be chemically separated.^{6,7} Additionally, in a collaboration with the Korean Advanced Institute of Science and Technology (KAIST), we are also currently undertaking a comparative study of the photochemistry, photoionization, and chemi-ionisation of individual stereoisomers using 1,2-dibromoethylene (DBE) as a prototypical system.⁸ These investigations aim to gain a comprehensive understanding of the role of molecular conformations in unimolecular and bimolecular reactivity.

¹ Willitsch, S. *Chemistry With Controlled Ions*, 1st ed., John Wiley & Sons: NJ 07030, USA, 1-342, 2017.

² Chang I, -Y. P. *et al.* Specific Chemical Reactivities of Spatially Separated 3-Aminophenol Conformers with Cold Ca⁺ Ions. *Science* 98, 342, 2013.

³ Kilaj I, A. *et al.* Conformer-specific polar cycloaddition of dibromobutadiene with trapped propene ions. *Nat. Commun.* 12, 6047, 2021.

⁴ Ploenes I, L. *et al.* A novel crossed-molecular-beam experiment for investigating reactions of state- and conformationally selected strong-field-seeking molecules. *Mol. Phys.* 119, 1965234, 2021.

⁵ Ploenes I, L. *et al.* *in prep.* 2023.

⁶ Shi I, W. *et al.* Rydberg spectra of *cis*-1,2-dibromoethylene. *Mol. Phys.* 105, 1701–1709, 2007.

⁷ Yamamoto I, T. *et al.* The Importance of Lone Pair Electron Delocalization in the *cis*–*trans* Isomers of 1,2-Dibromoethenes. *Chem. Lett.* 34, 8, 2005.

⁸ Kim I, J. *et al.* Multiphoton-excited dynamics of the *trans* or *cis* structural isomer of 1,2-dibromoethylene. *J. Chem. Phys.* 155, 164304, 2021.

Investigating Microdroplet Reactions Using Cryogenic Ion Vibrational Spectroscopy

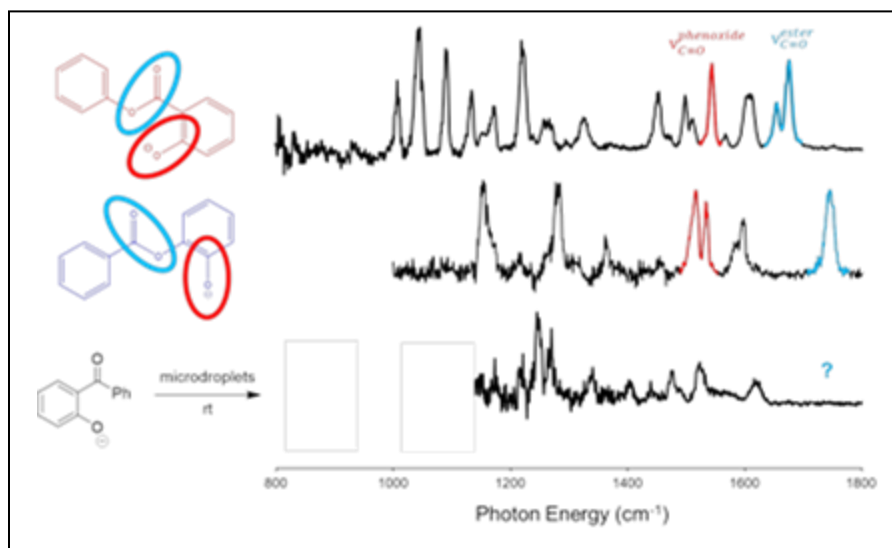
Ahmed Mohamed,^a Tim Schleif,^a Thien Khuu,^a Anasthasia Shilov,^a Jesús Valdiviezo,^b
Teresa Head-Gordon^b and Mark A. Johnson^a

^aDepartment of Chemistry, Yale University, 225 Prospect Street New Haven, CT 06511, USA
Email: a.mohamed@yale.edu

^bCollege of Chemistry, University of California, Berkeley, CA 94720, USA

ABSTRACT

Organic reactions carried out in microdroplets are accelerated compared to their bulk-phase counterparts. This remarkable phenomenon is attributed to the unique environment of the microdroplet. At the air-water interface, partial solvation of the reagents reduces the solvent reorganization energy and the increased surface area-to-volume ratio leads to high surface concentrations. Additionally, extraordinary pH conditions lead to the formation of products that otherwise require catalysts and heating to synthesize in the bulk phase. While promising for the future of small-scale synthesis, all mechanistic investigations of microdroplet reactions have been restricted by the limitations of mass spectrometry (MS). Although MS/MS provides fragmentation patterns that can be used to identify the presence of structural motifs, it falls short of providing unequivocal evidence of molecular connectivity.



We employ cryogenic ion vibrational spectroscopy (CIVS) to study two previously reported reactions carried out in microdroplets: Baeyer-Villiger (BV) oxidation of 2-hydroxybenzophenone and the nucleophilic addition of protonated formic acid to 1,2-diaminobenzene to produce benzimidazole. In the case of BV oxidation, CIVS reveals that the reported product does not share the same structure as that produced via electrospray ionization. For nucleophilic addition, CIVS reveals that benzimidazole is produced in the microdroplet. Additionally, we employ cluster chemistry to identify the size in which formic acid becomes protonated and a potential intermediate along the reaction pathway. These two cases demonstrate that spectroscopy is necessary in order to assign structures and invoke mechanism in microdroplet synthesis.

Capture, Angular Acceleration, and Release of CO₂ and CO in a Tunable Optical Centrifuge

Hannah M. Ogden, Tara J. Michael, Matthew R. Laskowski, and Amy S. Mullin

Department of Chemistry and Biochemistry, University of Maryland, College Park, USA

Email: mullin@umd.edu

ABSTRACT

The capture, angular acceleration, and release of CO₂ and CO molecules in a tunable optical centrifuge spectrometer were investigated using high-resolution transient IR absorption spectroscopy to elucidate the mechanisms by which an optical centrifuge ramps molecules into extreme rotational states. A tunable optical centrifuge uses ultrafast, oppositely-chirped laser pulses with tunable bandwidth to trap and angularly accelerate molecules into selected rotational states. Centrifuged molecules are released from the trap when the interaction energy between the optical field and the molecule is insufficient to drive them into the next higher rotational state. Reducing the optical bandwidth of the chirped pulses reduces the effective angular frequency Ω_{OC} of the optical trap, and enables control of the ultimate angular acceleration of the molecules, leading to molecules with lower rotational frequencies Ω_f .

Here, the nascent distributions for CO ($J=41-49$) and CO₂ ($J=200-240$) were measured as a function of the optical centrifuge bandwidth under low pressure conditions. A series of “clipped” optical centrifuge traps, as shown in Figure 1, were used to prepare molecules with classic rotational frequencies of $\Omega_f=3-3.6 \times 10^{13}$ radians s⁻¹. Transient fingerprint spectroscopy was used to identify new IR frequencies for CO₂ (00^01-00^00) ν_3 R-branch transitions with $J=200-240$. Number densities for the nascent CO and CO₂ distributions were used to characterize capture and acceleration efficiencies. The molecular aspects of the capture and acceleration are elucidated. The nascent distributions undergo collisional decay, and the Clip 3 time-dependent data were analyzed to determine rotational energy transfer rate constants for CO ($J>40$) and CO₂ ($J>200$). The results are compared to previous CO and CO₂ studies to elucidate the dynamics of molecules with large amounts of rotational energy.¹⁻⁴ This work is supported by the National Science Foundation.

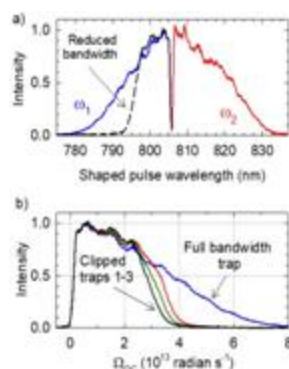


Figure 1. a) Chirped pulse spectra. b) Profiles of the optical centrifuge trap using full and reduced bandwidth pulses.

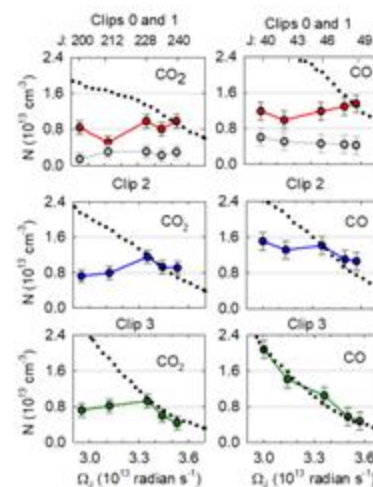


Figure 2. Transient IR absorption signals at 100 ns as a function the clipped optical trap.

¹ M. J. Murray, H. M. Ogden, C. Toro, Q. Liu and A. S. Mullin, Impulsive collision dynamics of CO super rotors from an optical centrifuge, *Chem Phys Chem* 17, 3692, 2016.

² M. J. Murray, H. M. Ogden, C. Toro, Q. Liu, D. A. Burns, M. H. Alexander and A. S. Mullin, State-specific collision dynamics of molecular super rotors with oriented angular momentum, *J. Phys. Chem. A* 119, 12471, 2015.

³ Tara J. Michael, Hannah M. Ogden, State-resolved rotational distributions and collision dynamics of CO made in a tunable optical centrifuge. *J. Chem. Phys.* 154, 134307, 2021.

⁴ M. R. Laskowski, H. M. Ogden, Tara J. Michael, and Amy S. Mullin, Rotational Energy Transfer Kinetics of Optically Centrifuged CO Molecules Investigated through Transient IR Spectroscopy and Master Equation Simulations. *Faraday Discussions* 238, 87, 2022.

Theoretical insights into the $\text{Cl}^- + \text{CH}_3\text{I}$ and the $\text{F}^- + \text{CF}_3\text{CH}_2\text{I}$ reactions

András Bence Nacsa, Viktor Tajti and Gábor Czakó

MTA-SZTE Lendület Computational Reaction Dynamics Research Group, Interdisciplinary Excellence Centre and Department of Physical Chemistry and Materials Science, University of Szeged, Szeged, Hungary. E-mail: nacsa.andras.bence@gmail.com

ABSTRACT

For the $\text{Cl}^- + \text{CH}_3\text{I}$ reaction, we have developed a full-dimensional *ab initio* potential energy surface (PES)¹ using a composite method, defined as $\text{CCSD-F12b} + \text{BCCD(T)} - \text{BCCD}$, with the aug-cc-pVTZ(-PP) basis set. The fitting was done by the permutationally-invariant polynomial approach. For an initial data set, we randomly displaced the previously-determined stationary points of the PES and fit an initial PES, later did further refinement with the ROBOSURFER program system, which improves the accuracy by iteratively adding points to the fitting set. The quasi-classical trajectory (QCT) simulations on the final PES showed two product channels to be active in our collision energy (E_{coll} , 1–80 kcal/mol) range: the $\text{S}_{\text{N}}2$ reactions leading to $\text{I}^- + \text{CH}_3\text{Cl}$ and iodine abstraction resulting in the $\text{ICl}^- + \text{CH}_3$ products. Detailed analysis of more than 1.5 million trajectories (reaction probabilities, integral cross sections, scattering angle, initial attack angle, product translational energy and product internal energy distributions) gave us deeper insights into the dynamics and mechanisms of the $\text{Cl}^- + \text{CH}_3\text{I}$ reaction. Finally, we could compare our results with crossed-beam experiments and previous direct dynamics simulations, and quantitative and/or qualitative agreement could be observed.

We also investigated the $\text{F}^- + \text{CF}_3\text{CH}_2\text{I}$ 9-atomic reaction.² The $\text{F}^- + \text{CH}_3\text{CH}_2\text{I}$ reaction has already been studied, however substituting the three hydrogen atoms with fluorine atoms can drastically change the reaction dynamics as the bimolecular elimination (E2) reaction pathway will be blocked. The stationary points of the PES were characterized at the $\text{CCSD(T)-F12a/cc-pVDZ(-PP)-F12}$ level of theory and we started a PES development. However, the *ab initio* computations at the randomly displaced points mostly did not converge, so we utilized a recently-developed method, ManyHF, which solves most of the convergence problems occurring during the creation of the initial data set.

¹ András B. Nacsa, Viktor Taiti, Gábor Czakó. Dynamics of the $\text{Cl}^- + \text{CH}_3\text{I}$ reaction on a high-level *ab initio* analytical potential energy surface. *J. Chem. Phys.* 158, 194306, 2023.

² Thomas Gstir *et al.* The influence of fluorination on the dynamics of the $\text{F}^- + \text{CF}_3\text{CH}_2\text{I}$ reaction. *Phys. Chem. Chem. Phys.* submitted, 2023.

Spontaneous N₂ cleavage under cryo conditions

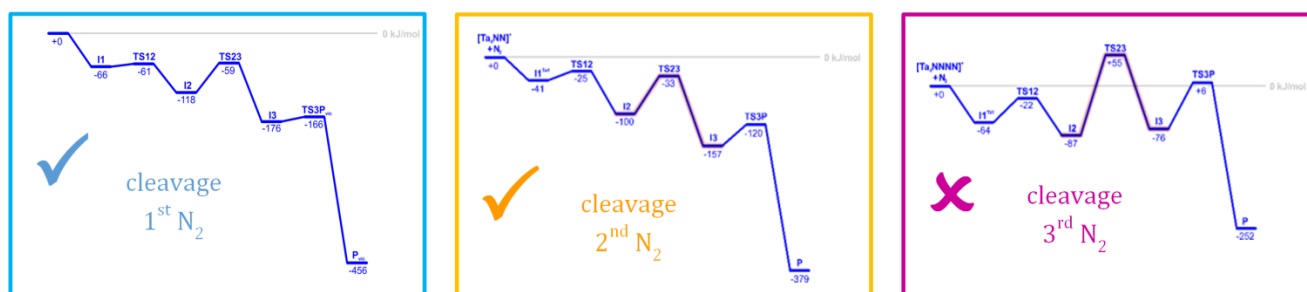
Gereon Niedner-Schatteburg

RPTU Kaiserslautern-Landau, Department of Chemistry, 67663 Kaiserslautern, Germany

Email: gns@chemie.uni-kl.de

ABSTRACT

Our research revealed cases of spontaneous N₂ cleavage without further activation. This was achieved by some naked transition metal (TM) clusters under cryo conditions within an ion trap. Choice of TM, of cluster size, and of cluster charge turned out crucial. We find this cleavage mediated by some cationic clusters, and by some anionic clusters. Most noteworthy, we find cases where the adsorption of multiple N₂ hampers activation – self poisoning – and cases where it enables the activation – self promotion. We embed these investigations into a long standing scheme of concerted studies that combine reaction kinetics, IR spectroscopy, electronic spectroscopy, and reaction path modeling by DFT quantum chemistry.^{1–13}



¹ GNS. in Structure and Bonding Vol. 174, 1-40, Springer, 2017.

² Dillinger, S. & GNS. in Fundamentals and Applications of Fourier Transform Mass Spectrometry, Elsevier, 2019.

³ Mohrbach, J., Dillinger, S., and GNS. Cryo Kinetics and Spectroscopy of cationic nickel clusters: Rough and smooth surfaces. *J. Phys. Chem. C* 121, 10907, 2017.

⁴ Mohrbach, J., Dillinger, S. & GNS. Probing cluster surface morphology by cryo kinetics of N₂ on cationic nickel clusters. *J. Chem. Phys.* 147, 184304, 2017.

⁵ Ehrhard, A. A., Klein, M. P., Mohrbach, J., Dillinger, S. & GNS. Cryokinetics and spin quenching in the N₂ adsorption onto rhodium cluster cations. *Mol. Phys.* 119, 1953172, 2021.

⁶ Straßner, A., Klein, M. P., Fries, D. V., Wiehn, C., Huber, M. E., Mohrbach, J., Dillinger, S., Spelsberg, D., Armentrout, P. B. & GNS. Kinetics of stepwise nitrogen adsorption by size-selected iron cluster cations: Evidence for size-dependent nitrogen phobia. *J. Chem. Phys.* 155, 244306, 2021.

⁷ Ehrhard, A. A., Klein, M. P., Mohrbach, J., Dillinger, S. & GNS. Cryo kinetics of N₂ adsorption onto bimetallic rhodium-iron clusters in isolation. *J. Chem. Phys.* 156, 05430, 2022.

⁸ Klein, M. P., Ehrhard, A. A., Mohrbach, J., Dillinger, S. & GNS. Infrared Spectroscopic Investigation of Structures and N₂ Adsorption Induced Relaxations of Isolated Rhodium Clusters. *Topics in Catalysis* 61, 106, 2018.

⁹ Dillinger, S., Mohrbach, J. & GNS. Probing cluster surface morphology by cryo spectroscopy of N₂ on cationic nickel clusters. *J. Chem. Phys.* 147, 184305, 2017.

¹⁰ Dillinger, S., Klein, M. P., Steiner, A., McDonald, D. C., Duncan, M. A., Kappes, M. M. & GNS. Cryo IR Spectroscopy of N₂ and H₂ on Ru₈⁺: The Effect of N₂ on the H-Migration. *J. Phys. Chem. Lett.* 9, 914, 2018.

¹¹ Fries, D. V., Klein, M. P., Steiner, A., Prosenc, M. H. & GNS. Observation and mechanism of cryo N₂ cleavage by a tantalum cluster. *Phys. Chem. Chem. Phys.* 23, 11345, 2021.

¹² Straßner, A., Wiehn, C., Klein, M. P., Fries, D. V., Dillinger, S., Mohrbach, J., Prosenc, M. H., Armentrout, P. B. & GNS. Cryo spectroscopy of N₂ on cationic iron clusters. *J. Chem. Phys.* 155, 244305, 2021.

¹³ Klein, M. P., Ehrhard, A. A., Huber, M. E., Straßner, A., Fries, D. V., Dillinger, S., Mohrbach, J. & GNS. Cryo infrared spectroscopy of N₂ adsorption onto bimetallic rhodium-iron clusters in isolation. *J. Chem. Phys.* 156, 014302, 2022.

Spin-orbit changing collisions of highly vibrationally excited NO molecules

Chatura A. Perera,^a Hua Guo^b and Arthur G. Suits^{a*}

^a *Department of Chemistry, University of Missouri, Columbia MO 65211, USA.*

Email: capq9y@umsystem.edu

^b *Department of Chemistry and Chemical Biology, University of New Mexico, Albuquerque, New Mexico 87131, USA*

ABSTRACT

Collision studies involving the open shell nitric oxide (NO) molecule have been central in many detailed investigations of molecular reaction dynamics as a prototype system for probing inelastic collisions. These processes have proven a powerful means of investigating molecular interactions, and much current effort is focused on the cold and ultracold regime where quantum phenomena are clearly manifested. Here I present our recent work on state-to-state spin-orbit changing collisions of highly vibrationally excited NO molecules prepared in single rotational and parity levels at $v=10$ using stimulated emission pumping (SEP).¹ This state preparation is employed in a near-copropagating beam geometry that permits very wide tuning of the collision energy, from far above room temperature down to 2 K where we test the theoretical treatment of the attractive part of the potential and the difference potential for the first time. We have obtained differential cross sections for state-to-state collisions of NO($v=10$) with Ar/Ne in spin-orbit excited manifold using velocity map imaging.² Overall good agreement of the experimental results was seen with quantum mechanical close-coupling calculations done on coupled-cluster potential energy surfaces. Probing cold collisions of NO carrying ~ 2 eV of vibrational excitation allows us to test state-of-the-art theory in this extreme nonequilibrium regime. The current experimental setup is now modified to permit a near-counterpropagating geometry for the molecular beams which allows us to look into really high collision energies to study chemistry in high temperature hypersonic flows. This takes us to a new direction where vibrationally inelastic processes may appear and the latest results along these experiments will also be presented.

(1) Perera, C. A.; Zuo, J.; Guo, H.; Suits, A. G. Differential Cross Sections for Cold, State-to-State Spin-Orbit Changing Collisions of No($V = 10$) with Neon. *The Journal of Physical Chemistry A* **2022**, *126* (21), 3338-3346.

(2) Amarasinghe, C.; Perera, C. A.; Li, H.; Zuo, J.; Besemer, M.; van der Avoird, A.; Groenenboom, G. C.; Guo, H.; Suits, A. G. Collision-Induced Spin-Orbit Relaxation of Highly Vibrationally Excited No near 1 K. *Natural Sciences* **2022**, *2* (1), e20210074.

Unimolecular decay dynamics of the simplest Criegee intermediate to OH products

Yujie Qian and Marsha I. Lester

Department of Chemistry, University of Pennsylvania, Philadelphia, PA 19104-6323, USA

Email: yq26@sas.upenn.edu

ABSTRACT

The simplest Criegee intermediate, formaldehyde oxide (CH_2OO), is produced by ozonolysis of terminal alkenes in the troposphere, where its unimolecular decay leads to hydroxyl (OH) radicals and other products. Isolated and jet-cooled CH_2OO prepared in the laboratory is characterized by IR action spectroscopy with time-resolved UV laser-induced fluorescence detection of the OH radical products. The IR action spectrum of CH_2OO is obtained in the overtone CH stretch region ($5940\text{--}6280\text{ cm}^{-1}$). The observed vibrational features and relative intensities are in good agreement with computed anharmonic frequencies and intensities. The IR excitation energies ($17.0\text{--}17.4\text{ kcal mol}^{-1}$) are below the transition state (TS) barrier *via* 1,3 ring closure ($19.1\text{ kcal mol}^{-1}$) predicted at a high level of theory.¹ As a result, the unimolecular decay of CH_2OO to OH products proceeds exclusively by quantum mechanical tunneling, specifically heavy-atom tunneling associated with ring closure. Experimental measurements reveal a relatively slow rate for appearance of OH products, which is compared with calculated Rice-Ramsperger-Kassel-Marcus energy-dependent rates $k(E)$ implemented with 1D Eckart tunneling. The latter is extended to thermal rate calculations $k(T,P)$ and compared with prior kinetic studies on unimolecular decay of CH_2OO under thermal conditions.²

¹ Nguyen, T. L. *et al.* Stabilization of the Simplest Criegee Intermediate from the Reaction between Ozone and Ethylene: A High-Level Quantum Chemical and Kinetic Analysis of Ozonolysis. *J. Phys. Chem. A*, 119 (22), 5524-5533, 2015.

² Peltola, J. *et al.* Time-resolved, broadband UV-absorption spectrometry measurements of Criegee intermediate kinetics using a new photolytic precursor: unimolecular decomposition of CH_2OO and its reaction with formic acid. *Phys. Chem. Chem. Phys.* 22 (21), 11797-11808, 2020.

Vibrational energy levels and predissociation lifetimes of the $A^2\Sigma^+$ state of SH/SD radicals by photodissociation spectroscopy

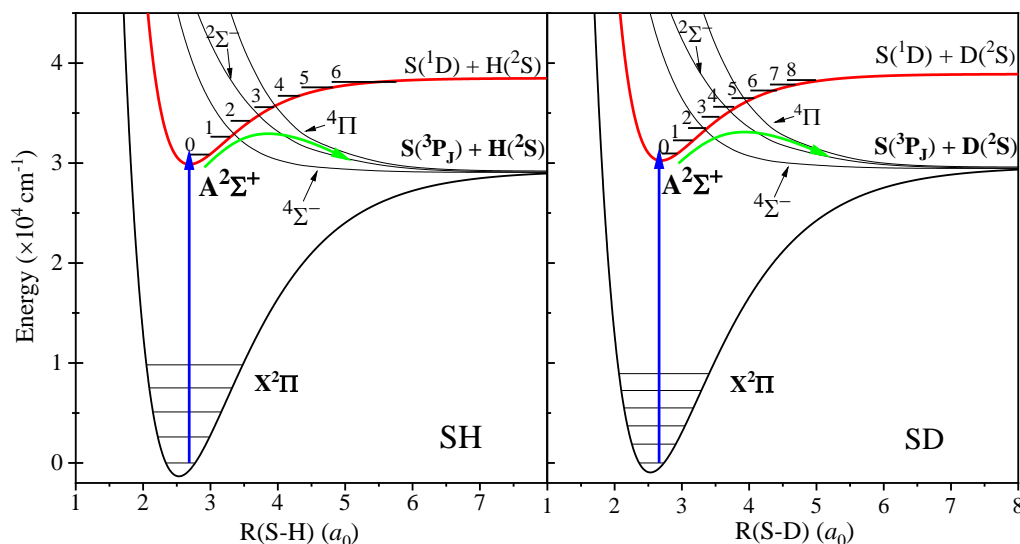
Yuan Qin, Xianfeng Zheng, Yu Song, Ge Sun and Jingsong Zhang

Department of Chemistry, University of California Riverside, Riverside, California 92521, USA

Email: yuan.qin@email.ucr.edu

ABSTRACT

Photo-predissociation of SH and SD radicals in the $A^2\Sigma^+$ state are investigated using the high- n Rydberg atom time-of-flight (HRTOF) technique.¹ By measuring the photoproduct translational energy distributions as a function of excitation wavelength, contributions from overlapping $A^2\Sigma^+ (v') \leftarrow X^2\Pi (v'')$ transitions can be separated, and the H/D + S(3P_J) photofragment yield (PFY) spectra are obtained across various rovibrational levels (SH $v' = 0-7$ and SD $v' = 0-8$) of the $A^2\Sigma^+ \leftarrow X^2\Pi$ bands. The upper $A^2\Sigma^+$ state vibrational levels $v' = 5-7$ of SH and $v' = 3-8$ of SD are determined for the first time. The PFY spectra are analyzed with the simulation program *PGOPHER*,² which gives vibrational origins and linewidths of the rovibrational levels of the $A^2\Sigma^+$ state. The linewidths ($\geq 1.5 \text{ cm}^{-1}$) of the SH $A^2\Sigma^+ v' = 3-7$ and SD $A^2\Sigma^+ v' = 2-8$ states are characterized for the first time in this work, demonstrating that these levels undergo rapid predissociation with lifetimes on the order of picosecond. The lifetimes of the SD $A^2\Sigma^+ v' = 0, N = 1$ and 2 levels are determined to be $247 \pm 50 \text{ ns}$ and $176 \pm 60 \text{ ns}$ by pump-probe delay measurements, respectively. The experimentally measured lifetimes are in a reasonable agreement with the theoretical predictions.



¹ Y. Qin, X. Zheng, Y. Song, G. Sun, and J. Zhang. Vibrational energy levels and predissociation lifetimes of the $A^2\Sigma^+$ state of SH/SD radicals by photodissociation spectroscopy. *J. Chem. Phys.* 157, 134303, 2022.

² C. M. Western. PGOPHER: A program for simulating rotational, vibrational and electronic spectra. *J. Quant. Spectrosc. Radiat. Transf.* 186, 221-242, 2017.

Two-photon dissociation dynamics of the mercapto radical

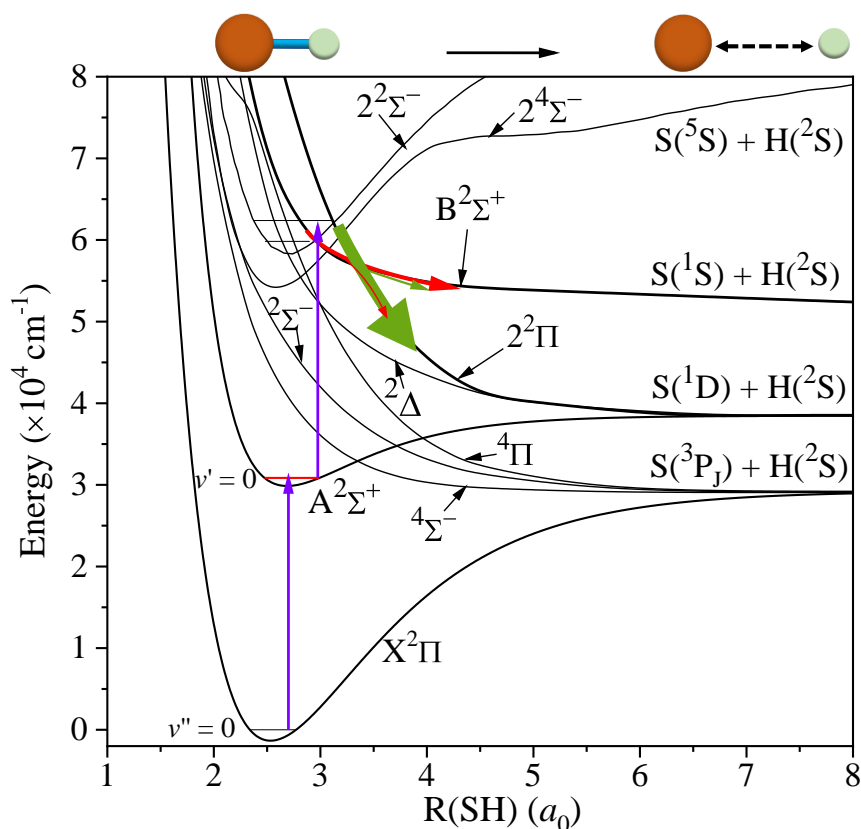
Yuan Qin, Xianfeng Zheng, Yu Song, Ge Sun and Jingsong Zhang

Department of Chemistry, University of California Riverside, Riverside, California 92521, USA

Email: yuan.qin@email.ucr.edu

ABSTRACT

Two-photon dissociation dynamics of the SH/SD radicals are investigated using the high- n Rydberg atom time-of-flight (HRTOF) technique.¹ The $\text{H/D}(^2\text{S}) + \text{S}(^1\text{D})$ and $\text{H/D}(^2\text{S}) + \text{S}(^1\text{S})$ products are observed in the dissociation of the SH/SD radicals on the $2^2\Pi$ and $\text{B}^2\Sigma^+$ repulsive states, from sequential two-photon excitation via the $\text{A}^2\Sigma^+$ ($v' = 0$, $J' = 0.5\text{--}2.5$) state. The angular distributions of both $\text{H/D}(^2\text{S}) + \text{S}(^1\text{D})$ and $\text{H/D}(^2\text{S}) + \text{S}(^1\text{S})$ product channels are anisotropic. The anisotropy parameter (β) of the $\text{H}(^2\text{S}) + \text{S}(^1\text{D})$ products is $\sim -0.8 \pm 0.1$ (-0.9 ± 0.05 for SD), and that of the $\text{H}(^2\text{S}) + \text{S}(^1\text{S})$ products is $\sim 1.3 \pm 0.3$ (1.2 for SD). The anisotropic angular distributions indicate that the SH/SD radicals promptly dissociate on the repulsive $2^2\Pi$ and $\text{B}^2\Sigma^+$ potential energy curves (PECs) along with some non-adiabatic crossings, leading to the $\text{H/D}(^2\text{S}) + \text{S}(^1\text{D})$ and $\text{H/D}(^2\text{S}) + \text{S}(^1\text{S})$ products, respectively. The bond dissociation energy of the ground-state $\text{X}^2\Pi_{3/2}$ SH/SD to the ground-state $\text{H/D}(^2\text{S}) + \text{S}(^3\text{P}_2)$ products is measured to be $D_0(\text{S-H}) = 29253 \pm 20 \text{ cm}^{-1}$ and $D_0(\text{S-D}) = 29650 \pm 20 \text{ cm}^{-1}$, respectively. The dissociation energy of the $\text{A}^2\Sigma^+$ state SH/SD to the $\text{H/D}(^2\text{S}) + \text{S}(^1\text{D})$ products is derived to be $D_0[\text{S-H(A)}] = 7659 \pm 20 \text{ cm}^{-1}$ and $D_0[\text{S-D(A)}] = 7940 \pm 20 \text{ cm}^{-1}$.



¹ Y. Qin, X. Zheng, Y. Song, G. Sun, and J. Zhang. Two-photon dissociation dynamics of the mercapto radical. *Phys. Chem. Chem. Phys.* 24, 27232-27240, 2022.

Temperature- and Size-Dependent, Water-Cluster-Mediated Long Range Proton Transfer in Microhydrated 4-Aminobenzoic Acid

Abhijit Rana,^a Thien Khuu,^a Santino J. Stropoli,^a Sean C. Edington,^a Tae Hoon Choi,^b
Kenneth D. Jordan,^b B. Anne McCoy^c and Mark A. Johnson^a

^a*Sterling Chemistry Laboratory, Yale University, New Haven, CT, 06520, USA*

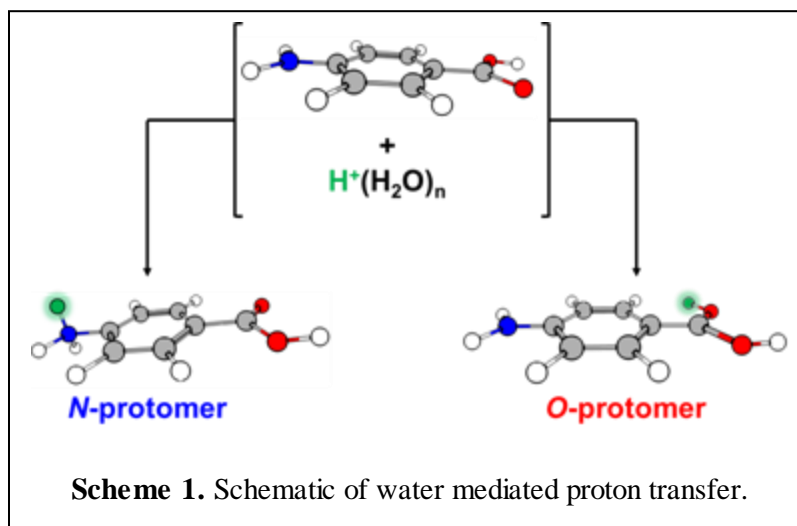
Email: abhijit.rana@yale.edu

^b*Department of Chemistry, University of Pittsburgh, Pittsburgh, PA, 15260, USA*

^c*Department of Chemistry, University of Washington, Seattle, WA, 98195, USA*

ABSTRACT

We explore water-mediated proton transfer between two spectroscopically distinct protonation sites adopted by 4-aminobenzoic acid (4ABA). This is achieved by following the spectroscopic behavior of $\text{H}^+\text{-4ABA}\cdot(\text{H}_2\text{O})_{n=0-4}$ cluster ions held in a temperature-controlled ion trap. Protonation occurs at the acid (*O*-protomer) and amine (*N*-protomer) functionalities, which display dramatically different ultraviolet (UV) absorption bands. After most of the *O*-protomer population is depleted by UV excitation with a 6 ns pulse width laser near 310 nm, we record time evolution of the protomer populations over tens of milliseconds by monitoring the characteristic vibrational bands of two protomers. Temperature-dependent interconversion with retention of the water molecules is observed for $n = 3$ and 4 but not $n = 2$. These results thus support an earlier theoretical prediction that the transfer mechanism changes from $n = 2$ to 3.



Exploring New High Energy Rotational States of N₂O with a Tunable Optical Centrifuge

Michael E. Ritter, Christopher R. Lukowski, Simone A. DeSouza and Amy S. Mullin

Department of Chemistry and Biochemistry, University of Maryland, College Park, USA
Email: meritter@umd.edu

ABSTRACT

A tunable optical centrifuge is used to investigate high rotational energy states of N₂O that have not previously been reported. A full-bandwidth optical centrifuge angularly accelerates N₂O molecules to rotational states as high as J=380. Tuning the optical centrifuge is accomplished by reducing the spectral bandwidth, thereby lowering the rotational states of molecules that are released from the optical trap, as shown in Figure 1. Population in selected states is optimized by tuning the optical centrifuge bandwidth to correspond to selected rotational frequencies. High-resolution transient IR absorption spectroscopy is used to probe rotationally-resolved transition frequencies of the N₂O (00⁰1-00⁰0) band at $\lambda=4.4\ \mu\text{m}$. Prior to our studies, IR transitions from the (00⁰0) state had been reported up to J=92 in long path absorption measurements¹. The selectivity of the tunable optical centrifuge enables us to observe nearly all N₂O R-branch rotational transitions with J=100-205 and P-branch transitions up to J=135, based on the tuning range of the IR probe lasers. Figure 1 shows a four-fold enhancement in transient absorption signals at t=300 ns for the R134 transition when the optical centrifuge bandwidth is reduced. This work expands on previous IR measurements from our group of a number of N₂O R-branch transitions using a tunable optical centrifuge between J=93 and 205^{2,3}.

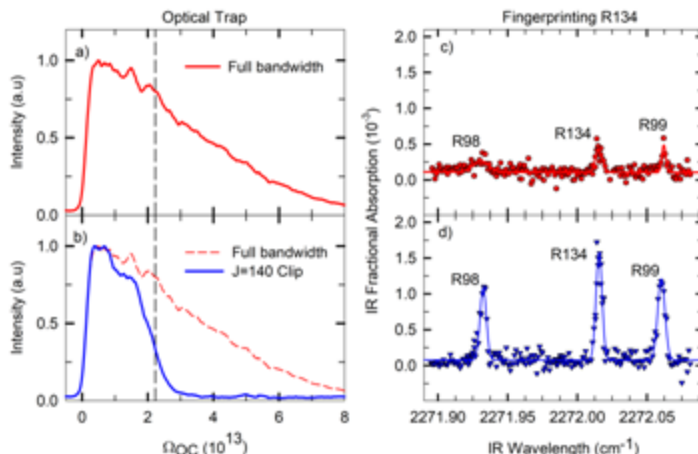


Figure 1. Optimizing population for IR transitions of N₂O J=100-205. a) Full bandwidth optical centrifuge trap and b) optical centrifuge trap optimized for J=140. c) Transient IR fingerprint spectrum at t=300 ns for the N₂O R134 transition using the full bandwidth optical trap. d) Fingerprint spectrum with the optimized optical trap.

The experimental results are compared to two models. In the first model, rotational energies for N₂O (00⁰0) and (00⁰1) up to J=205 are extrapolated using a third-order expansion of the rigid rotor model and low-J spectral constants reported by Toth¹. The second model by Perevalov and coworkers is semi-empirical and uses an effective Hamiltonian that includes rotationally resolved polyads of more than 40 vibrational modes⁴. The observed R200 transition frequency is within 0.05 cm⁻¹ of the first model and within 0.021 cm⁻¹ of the second model. Finally, rotational energies for the (00⁰0) vibrational state up to J=134 and the (00⁰1) vibrational state up to J=135 are determined using combination differences and results are compared to the models. This study lays the groundwork for identifying new probe transitions for J=250-380 that will be used in future dynamics studies.

¹ Toth, R. A. Line-Frequency Measurements and Analysis of N₂O between 900 and 4700cm⁻¹. *Applied Optics*, 30, 5289, 1991..

² Yuan, L., et al. Dynamics of Molecules in Extreme Rotational States, *Proc. Natl. Acad. Sci.*, 108, 6872–6877, 2011.

³ Oden, H., et al. Transient IR (0001–0000) Absorption Spectroscopy of Optically Centrifuged N₂O with Extreme Rotation up to J = 205. *J. Quant. Spectrosc. Radiat. Transf.*, 246, 106867, 2020.

⁴ Perevalov, V. I., et al. Global Modeling of the ¹⁴N₂¹⁶O Line Positions within the Framework of the Polyad Model of Effective Hamiltonian. *J. Quant. Spectrosc. Radiat. Transf.*, 113 (11), 1004–1012, 2012.

Nonadiabatic Dynamics with Only Potential Energies and Gradients

Yinan Shu,^a Linyao Zhang^b and Donald G. Truhlar^a

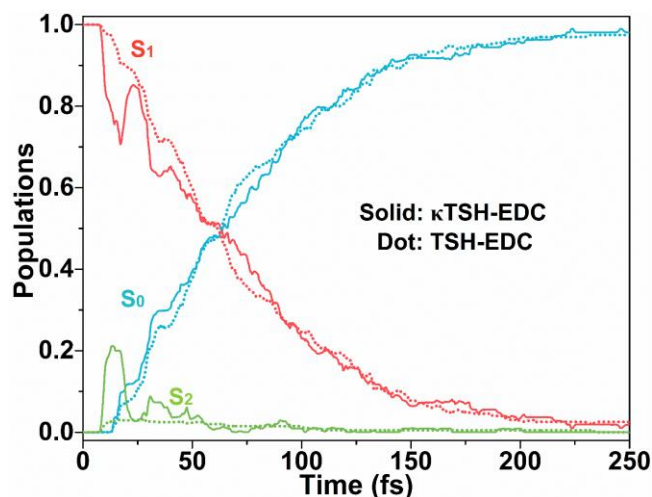
^a Department of Chemistry, University of Minnesota, Minneapolis, MN 55455-0431, USA

Email: yinan.shu.0728@gmail.com

^b School of Energy Science and Engineering, Harbin Institute of Technology, Harbin, 150001, China

ABSTRACT

We often employ mixed-quantum classical (MQC) algorithms to simulate nonadiabatic processes involve multiple electronic states. There are in general two categories of MQC algorithms, namely, trajectory surface hopping (TSH), and self-consistent potential (SCP) methods. The electronic equation of motion (EOM) of TSH and SCP methods involve nonadiabatic coupling vector (NACs) terms that can be expressed as time derivative couplings (TDCs). While the nuclear EOM of SCP methods involves terms that are explicitly in NACs. Evaluating NACs from the electronic structure theory is cumbersome, for reasons that the number of NACs scales quadratically with the number of electronic states and therefore it is expensive to evaluate, and it limits the possible electronic structure theories that MQC algorithms can be interfaced with. One can address this issue partly in TSH by evaluating TDCs from overlap integrals of electronic wave functions at successive time steps. However, such approach still requires wave functions to be available for electronic structure theory. In addition, this advantage cannot be fully utilized for SCP methods because it requires an explicit evaluation of NACs. In this talk, I will introduce the recent development on how we circumvent such difficulty by accurately approximate TDCs from the information of only potential energies and gradients, and therefore, one can propagate accurate nonadiabatic dynamics without evaluating NACs or overlap integrals (which are often used to approximate TDCs). This new category of MQC algorithm is called curvature-driven algorithm.^{1,2} Not only the curvature-driven algorithms are more efficient without losing accuracy,¹ but also can be interfaced with electronic structure theories for which the wave functions are not available (and therefore one cannot evaluate TDCs from overlap integrals). The latter involves many popular machine learning electronic structure methods and multi-state pair density functional theories. Specifically, I will show you how to apply this curvature approximation to TSH and coherent switching with decay of mixing (CSDM), and the result methods are called κ TSH and κ CSDM. And how to extend these methods to simulate both internal conversion and intersystem crossing processes.



¹ Shu, Y.; Zhang, L.; Sun, S.; Truhlar, D. G. Time-Derivative Couplings for Self-Consistent Electronically Nonadiabatic Dynamics. *J. Chem. Theory Comput.* 16, 4098-4106, 2020.

² Shu, Y.; Zhang, L.; Chen, X.; Sun, S.; Huang, Y.; Truhlar, D. G. Nonadiabatic Dynamics Algorithms with Only Potential Energies and Gradients: Curvature-Driven Coherent Switching with Decay of Mixing and Curvature-Driven Trajectory Surface Hopping. *J. Chem. Theory Comput.* 18, 1320-1328, 2022.

³ Zhang, L.; Shu, Y.; Bhaumik, S.; Chen, X.; Sun, S.; Huang, Y.; Truhlar, D. G. Nonadiabatic Dynamics of 1,3-Cyclohexadiene by Curvature-Driven Coherent Switching with Decay of Mixing. *J. Chem. Theory Comput.* 18, 7073-7081, 2022.

Complex-valued potential energy surfaces for studying Penning ionization reaction

Wojciech Skomorowski

University of Warsaw, Centre of New Technologies, Banacha 2c, 02-097 Warsaw, Poland

Email: w.skomorowski@cent.uw.edu.pl

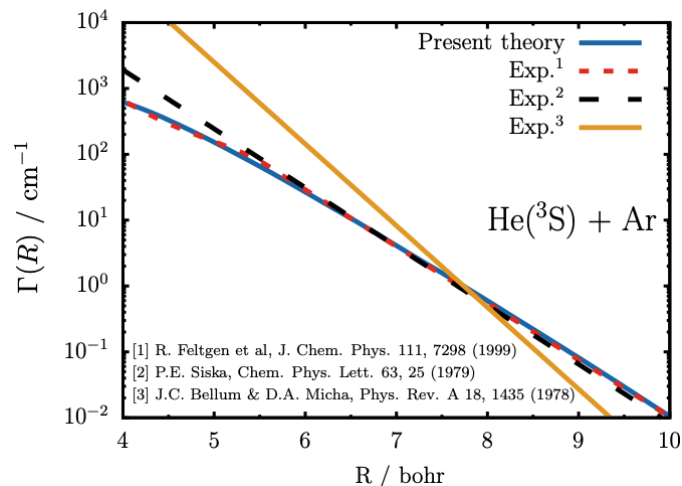
ABSTRACT

Penning ionization is a process of the general form:



in which target atom or molecule M is ionized by collision with electronically excited reagent A^* . Typically, A^* is a noble-gas atom in its excited metastable state, such as $\text{He}(^3\text{S})$ or $\text{Ne}(^3\text{P})$. The target M can be any atom or molecule as long as its lowest ionization potential is below the internal energy of A^* . Due to its unique characteristics, for many years Penning ionization has been the subject of significant experimental research by means of molecular beam techniques¹. In the past 10 years, several breakthrough experiments with Penning ionization have demonstrated how pure quantum phenomena can be observed in cold chemistry². Yet, despite the importance of Penning ionization reaction in many experimental settings and fundamental research, its first-principle modeling remains challenging, even for the smallest atomic/molecular systems. The major difficulty in theoretical description of this process arises from the autoionizing nature of the electronic state which governs the entrance channel of the reaction. If coupling with the electronic continuum is to be included within the framework of Born-Oppenheimer approximation, then complex-valued potential energy surfaces are needed.

Here we present a novel approach to calculate complex-valued optical potentials for molecular systems which undergo Penning ionization. Our method combines Fano-Feshbach resonance theory with equation-of-motion coupled-cluster (EOM-CCSD) wave function, and explicit description of the unbound electron. We show how to construct effectively Feshbach projectors within the EOM-CCSD framework, designed specifically to target systems undergoing Penning ionization. In the method we approximate state of the outgoing electron with a Coulomb wave, expanded in terms of auxiliary basis set composed of products of plane wave and Gaussian type orbitals. The proposed computational scheme is an extension of our recent work on calculating Auger decay rates in core-ionized/core-excited molecules³.



As a numerical illustration, we present complex-valued potential energy surfaces for a few benchmark systems such as $\text{He}(^3\text{S}) + \text{Ar}$, $\text{He}(^3\text{S}) + \text{H}_2$, or $\text{Ne}(^3\text{P}) + \text{Ar}$. The reported complex potentials are compared with available empirical surfaces derived from the experimental data. Presented method opens up a possibility for fully ab initio quantum-dynamical studies of Penning ionization reaction, even for systems containing sizable molecular targets.

¹ Siska P.E., Molecular-beam studies of Penning ionization. *Rev. Mod. Phys.* 65, 337, 1993.

² Klein A., A. *et al.* Directly probing anisotropy in atom-molecule collisions through quantum scattering resonances. *Nat. Phys.* 13, 35, 2017.

³ Skomorowski W. and Krylov A.I Feshbach-Fano approach for calculation of Auger decay rates using equation-of-motion coupled-cluster wave functions. I. Theory and implementation. *J. Chem. Phys.* 154, 084124, 2021.

Pushing the Limits of Anharmonic Vibrational Simulations Using Local Modes

Ryan Spencer,^a Emily Yang^b and Ryan P. Steele^c

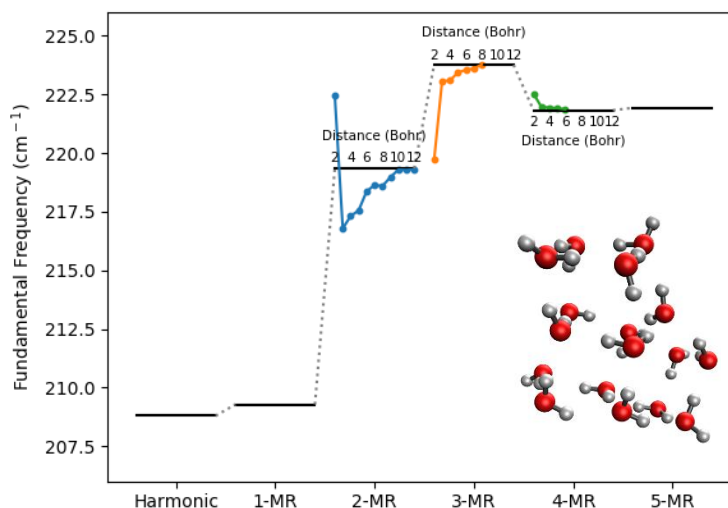
^a Steele, University of Utah, 315 S 1400 E Salt Lake City, UT 84112, USA
Email: u1217480@uemail.utah.edu

^b Steele, University of Utah, 315 S 1400 E Salt Lake City, UT 84112, USA

^c Chemistry, University of Utah, 315 S 1400 E Salt Lake City, UT 84112, USA

ABSTRACT

Vibrational spectroscopy is a powerful experimental tool that can be used to decipher the properties and potential energy surface for molecules and ensembles. Anharmonicity—deviation from the typical harmonic-oscillator reference picture—often indicates important details, such as strong hydrogen bonding, bond rearrangements, or even resonant vibrational interactions. These effects frequently differ from the results of often-used harmonic scaling factors, yet direct inclusion of such effects is often prohibitively costly compared to harmonic simulations, due to the need for inclusion of mode-coupling effects. Recent research in the Steele group has demonstrated the opportunity to examine molecular vibrations in a local-mode context,^{1,2,3} which allows for distance-based truncation of mode couplings and orders-of-magnitude acceleration of vibrational simulations. However, this approach has nonetheless been limited to heavily truncated versions of the so-called “n-mode representation”, wherein pairs, triples, etc., of modes are included in the vibrational potential. In this presentation, we demonstrate that heretofore-inaccessible convergence of this n-mode representation can be achieved within the local-mode picture, as shown in Figure 1 for a water-displacement motion in (H₂O)₁₇, thereby providing the possibility of fully converged, exact anharmonic simulations for molecules beyond small reference systems. In addition to these computational accelerations, such simulations provide new insight into the nature and distance dependence of the electronic coupling between vibrational motions.



¹ Xialou Cheng and Ryan P. Steele. Efficient anharmonic vibrational spectroscopy for large molecules using local-mode coordinates. *JCP* 141, 104105-104115, 2015.

² Xialou Cheng, *et al.* Tuning vibrational mode localization with frequency windowing. *JCP* 145, 124112-124124, 2016.

³ Thomas Weymuth, *et al.* A Local-Mode Model for Understanding the Dependence of the Extended Amide III Vibrations on Protein Secondary Structure. *JPCB* 114, 10649-10660, 2010.

Simulating Bimolecular Collisions with Machine Learning Potential

Kazuumi Fujioka, Allen Vincent and Rui Sun

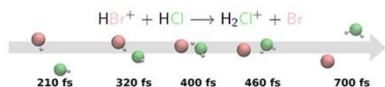
University of Hawaii, Manoa, Honolulu, Hawaii, USA. Email: ruisun@hawaii.edu

ABSTRACT

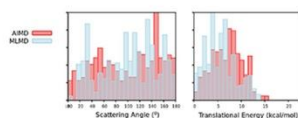
Machine learning has grown in use for constructing potential energy surfaces for their ability to theoretically recreate any function given enough training as well as their fast predictive powers after being trained. When trained on *ab initio* data, this enables simulation of an unprecedented number of *ab-initio*-quality trajectories. Herein, rigorous benchmarking of these machine-learned potential energy surfaces - both in terms of their static errors and dynamics errors - is carried out for two multi-product-channel ion-molecule bimolecular collisions ($\text{HBr}^+ + \text{HCl}$ and $\text{HBr}^+ + \text{CH}_4$). Comparison with *ab initio* molecular dynamics (AIMD) simulations provides one of the first direct evidence of ML potential's ability of recreating the dynamic, ensemble-average properties such as the cross section of the reaction, time of flight of the products, etc. It is also of interest to note that ML potential with smaller static error, identified with a limited size of the validations set, does not necessarily lead to better dynamic, ensemble-average properties in MLMD. Finally, once carefully calibrated, the large number of MLMD trajectories does not only provide better statistics, but they are also essential in applying other post-process techniques (e.g., zero-point energy restraint) that are critical to reach remarkable agreement with guided-beam experimental results.

Can ML Replicate AIMD and Model Experiments?

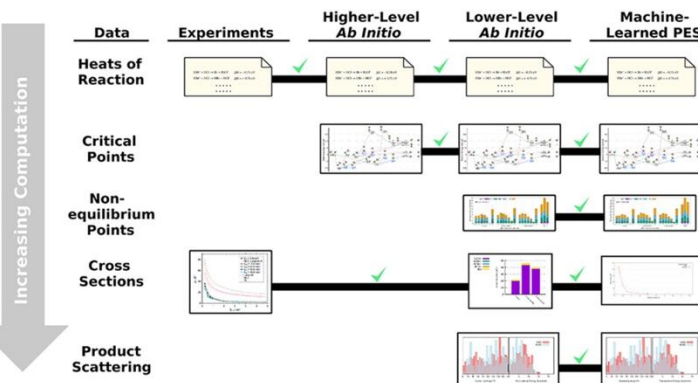
- Three machine-learning (ML) models recreate the potential energy surface (PES) of the reaction:



- Results from *ab initio* molecular dynamics (AIMD) are compared to the ML molecular dynamics



- Cross sections are replicated with the best ML model for collision energies unexplored by the AIMD



ML models are able to predict energies and energy gradients **orders of magnitude faster** than *ab initio* calculations, opening up possibilities for simulating very many or very long chemical reactions.



Quantum resonances in ultracold atom-ion and atom-molecule collisions

Michał Tomza

University of Warsaw, Poland. Email: michal.tomza@fuw.edu.pl

ABSTRACT

Cold and ultracold systems attract researchers' attention because the universe's quantum nature clearly manifests under such conditions, and research into such systems provides new insight into the quantum theory of matter and matter-light interaction. Ultracold atoms, ions, and molecules offer numerous exciting research prospects ranging from quantum-controlled chemical reactions and quantum simulations to precision spectroscopic measurements probing the fundamental laws of nature.

I will present our recent results of *ab initio* electronic structure and multichannel scattering calculations proposing, guiding, and explaining ultracold quantum physics experiments. I will start with our efforts related to hybrid systems of laser-cooled trapped ions and ultracold atoms combined in a single experimental setup. In collaboration with experimental groups in Amsterdam and in Freiburg, we reached and explained the quantum regime of ion-atom collisions manifested via shape resonances¹ and their quantum control with an external magnetic field observed with magnetic Feshbach resonances.² Giant second-order spin-orbit coupling is responsible for measured Feshbach resonances. I will conclude with explaining the mechanism³ of recently observed magnetic Feshbach resonances in ultracold atom-molecule mixtures.⁴ In collaboration with groups at MIT and in Nijmegen, we showed that these Feshbach resonances result from spin-rotation and spin-spin couplings in combination with the anisotropic atom-molecule interaction.³

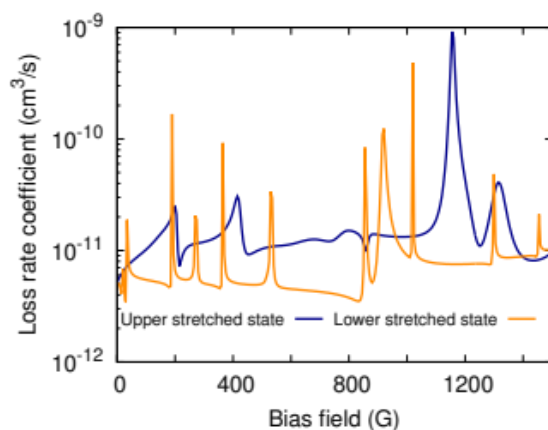


Figure 1: Theoretical prediction of magnetic Feshbach resonances in ultracold NaLi+Na collisions [3].

¹ T. Feldker, H. Fürst, H. Hirzler, N. V. Ewald, M. Mazzanti, D. Wiater, M. Tomza and R. Gerritsma, Buffer gas cooling of a trapped ion to the quantum regime, *Nature Phys.* 16, 413, 2020.

² P. Weckesser, F. Thielemann, D. Wiater, A. Wojciechowska, L. Karpa, K. Jachymski, M. Tomza, T. Walker and T. Schaetz, Observation of Feshbach resonances between a single ion and ultracold atoms, *Nature* 600, 429, 2021.

³ J. J. Park, H. Son, Y.K. Lu, T. Karman, M. Gronowski, M. Tomza, A. O. Jamison and W. Ketterle, Spectrum of Feshbach resonances in NaLi + Na collisions, submitted to *Phys. Rev. X* / arXiv:2303.00863, 2023.

⁴ H. Son, J. J. Park, Y.K. Lu, A. O. Jamison, T. Karman and W. Ketterle, Control of reactive collisions by quantum interference, *Science* 375, 1006, 2022.

Trapping and sympathetic cooling of conformationally selected ions

Lei Xu, Jutta Toscano and Stefan Willitsch

Department of Chemistry, University of Basel, Klingelbergstrasse 80, 4056 Basel, Switzerland

Email: jutta.toscano@unibas.ch

ABSTRACT

The different effective dipole moment of conformational isomers allows for their spatial separation by means of electrostatic deflection, enabling their individual reactivity to be investigated.¹ Recently, the conformer-specific polar cycloaddition of dibromobutadiene (DBB) with trapped propene ions has shown that both *gauche* and *s-trans* DBB conformers display capture-limited reaction rates.² The reaction was found to occur through both a concerted and a stepwise reaction mechanism, despite the spatial rearrangement of atoms necessary in *s-trans* DBB for the latter to take place. These results were obtained by selectively aiming the molecular beam containing either one of the two conformers at a static target of propene ions embedded within a laser-cooled Coulomb crystal of calcium ions. In order to gain further control over the reaction partners, we also wish to select the conformational isomer of the ionic reactant.

Here, we demonstrate for the first time the sympathetic cooling of different conformational isomers within a Coulomb crystal, setting the scene for fully conformationally selected ion–molecule reaction studies. Following the successful isomer-selective ionisation and loading of the two *m*-aminostyrene conformers into Coulomb crystals of trapped and laser-cooled calcium ions, we now aim to investigate their isomer-specific reactivity.

¹ Y.-P. Chang *et al.*, Specific Chemical Reactivities of Spatially Separated 3-Aminophenol Conformers with Cold Ca⁺ Ions, *Science* 342, 98, 2013.

² A. Kilaj *et al.*, Conformer-specific polar cycloaddition of dibromobutadiene with trapped propene ions, *Nat. Commun.* 12, 6047, 2021.

Trifluoromethane (CHF_3) Quantum Yields in the Pulsed Laser Photolysis of Trifluoroacetaldehyde (CF_3CHO) at 248, 266, 281, and 308 nm at Pressures between 100 and 650 Torr

Daniel Van Hoomissen,^{a,b} Aparajeo Chattopadhyay^{a,b} and James B Burkholder^b

^aCooperative Institute for Research in Environmental Sciences, University of Colorado Boulder, 216 UCB, Boulder, CO 80309, USA. Email: daniel.van-hoomissen@noaa.gov

^bChemical Sciences Laboratory, R/CSL5 National Oceanic and Atmospheric Administration (NOAA), 325 Broadway, Boulder, CO 80305-3328, USA. Email: james.b.burkholder@noaa.gov

ABSTRACT

Hydrofluoroolefins (HFOs), referred to as ‘fourth generation’ refrigerants, are being considered as replacements for chlorofluorocarbons (CFCs) and hydrofluorocarbons (HFCs). Compared to CFCs and HFCs, HFOs, in general, have lower global warming potentials (GWP) and zero ozone depletion potential (ODP). However, atmospheric degradation of HFOs containing the $\text{CF}_3\text{CH}_2=$ moiety can lead to the formation of trifluoroacetaldehyde (CF_3CHO). Upon UV photolysis, CF_3CHO has the potential to form trifluoromethane (CHF_3), a potent greenhouse gas (GWP=14,700 on the 100-year time horizon). Therefore, accurate measurement of quantum yields, $\phi(\lambda)$, in the UV photolysis CF_3CHO is critical for understanding its climate impacts.

This study directly quantifies $\phi_{\text{CHF}_3}(\lambda)$ and $\phi_{\text{CF}_3\text{CHO}}(\lambda)$ in the pulsed laser photolysis of CF_3CHO at 248, 266, 281, and 308 nm and pressures between 100 and 650 Torr (N_2/NO) using Fourier transform infrared spectroscopy (FTIR) and gas-chromatograph mass-spectrometry (GC/MS) detection methods. Our results indicate that photolysis of CF_3CHO at 308 nm, a tropospherically relevant photolysis wavelength, leads to a small, but measurable, $\phi_{\text{CHF}_3}(308 \text{ nm})$ of $\sim 10^{-4}$ at atmospheric pressure. Figure 1 illustrates the CF_3CHO quantum yield results measured in this work. The experimental methods, range of conditions, and interpretation of the $\phi_{\text{CHF}_3}(\lambda)$ and $\phi_{\text{CF}_3\text{CHO}}(\lambda)$ measurements will be discussed. The present results will be critically compared with previous indirect broadband photolysis, low-pressure, and theoretical studies of $\phi_{\text{CHF}_3}(\lambda)$ and $\phi_{\text{CF}_3\text{CHO}}(\lambda)$ to resolve existing discrepancies and limitations in previous studies.

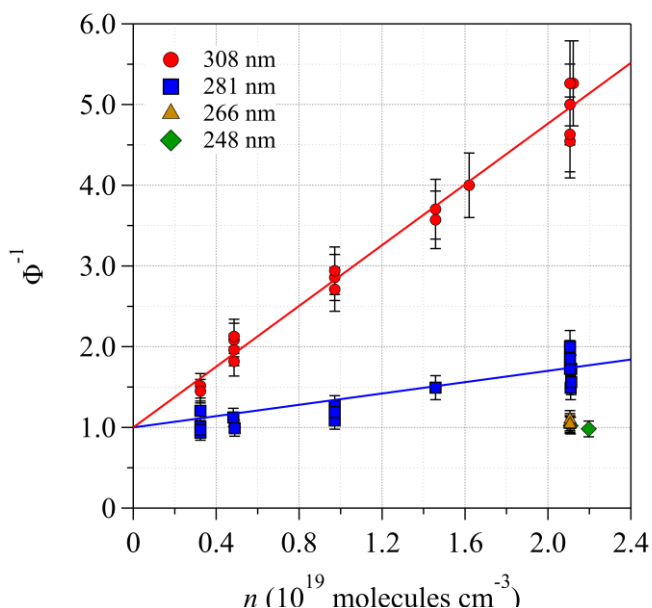


Figure 1. Stern-Volmer plot of CF_3CHO photolysis measured in this work at various wavelengths.

Direct Overtone Pumping and Vibrational Relaxation of CO₂

Pierce E. van Mulbregt, Raina M. Morley and Amy S. Mullin

Department of Chemistry and Biochemistry, University of Maryland, College Park, USA

Email: piercevm@umd.edu and rmorley@terpmail.umd.edu

ABSTRACT

This project investigates the state-resolved dynamics of vibrationally excited CO₂ prepared by direct overtone pumping. Vibrationally excited states populated by overtone excitation are important in Earth's atmosphere as they can contain enough energy to break chemical bonds and have relatively slow emission lifetimes.¹ Collisional relaxation competes with radiative decay, and the product energy partitioning into rotational and translational energies is determined by the energy transfer mechanisms. Previous studies have investigated the dynamics of overtone-excited C-H and O-H stretches, but less is known about CO₂.^{2,3,4} Here, two methods of overtone pumping are used to prepare the vibrationally excited molecules, as shown in Figure 1. In Scheme 1, the (1001) state is excited with a CW single-mode mid-IR OPO near $\lambda=2.7\ \mu\text{m}$. The pump beam is chopped for transient detection. In Scheme 2, the (1003) state is pumped by a pulsed near-IR OPO near $\lambda=1.2\ \mu\text{m}$. High-resolution transient IR absorption spectroscopy of one quantum of the ν_3 stretching mode near $\lambda=4.4\ \mu\text{m}$ is used to characterize the excitation and monitor the subsequent relaxation dynamics.

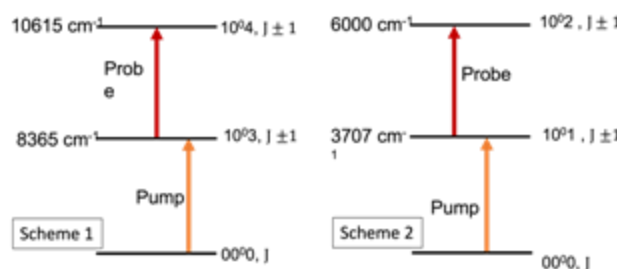


Figure 1. Schemes for CO₂ overtone excitation and transient IR absorption probing.

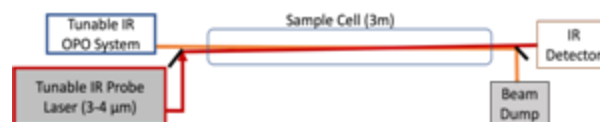


Figure 2. Experimental setup for overtone experiments.

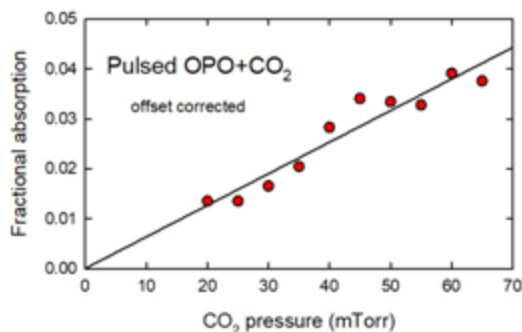


Figure 3. Window-loss offset corrected Pressure-dependent absorption of pump pulses to populate the CO₂ (10⁰₃) state.

the overtone-pumped states; and 3) Doppler-broadened line profiles to characterize the translational energy of the collision products. These studies will identify the major collisional relaxation pathways and provide insight into the role of vibrationally excited CO₂ molecules in hot environments.

¹ Veronica Vaida, *et al.* "Sunlight-Initiated Photochemistry: Excited Vibrational States of Atmospheric Chromophores", *International Journal of Photoenergy*, vol. 2008, Article ID 138091, 13 pages, 2008.

² Christopher G. Elles, *et al.* "Vibrational relaxation of CH₃I in the gas phase and in solution" *J. Chem. Phys.* 120, 6973–6979 (2004)

³ Amitabha Sinha, *et al.* "State- resolved unimolecular reactions: The vibrational overtone initiated decomposition of nitric acid." *J. Chem. Phys.* January 1990; 92 (1): 401–410..

⁴ Joann M. Pfeiffer, *et al.* "Probing the new bond in the vibrationally controlled bimolecular reaction of O with HOD(4vOH)." *J. Chem. Phys.* November 2000; 113 (18): 7982–7987.

Rigorous quantum calculations of rovibrational states of fluxional molecular complexes

P. Vindel-Zandbergen,^a D. Kedziera^b, M. Zoltowski^c, J. Klos^d, P. Zuchowski^b, P. Felker,^b
F. Lique^c and Z. Bačić^{a,f,g}

^a Department of Chemistry, New York University, New York, New York 10003, USA

^b Department of Chemistry, Nicolaus Copernicus University, 87-100 Toruń, Poland

^c Univ Rennes, CNRS, Institut de Physique de Rennes - UMR 6251, F-35000 Rennes, France

^d Joint Quantum Institute, University of Maryland, College Park, Maryland 20742, USA

^e Simons Center for Computational Physical Chemistry at New York University

^f NYU-ECNU Center for Comp. Chemistry at NYU Shanghai, Shanghai, 200062, China

^g Department of Chemistry and Biochemistry, University of California, Los Angeles, CA 90095-1569, USA

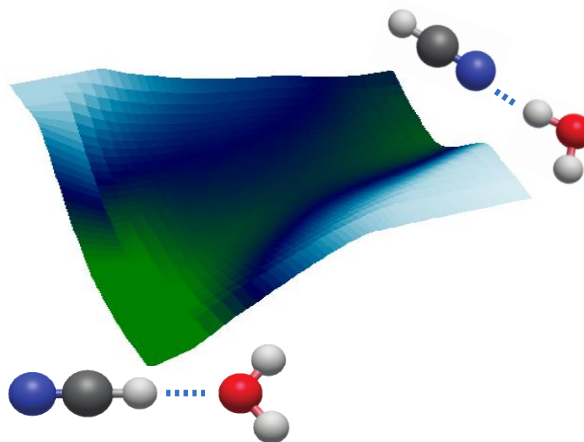
Email: patricia.vindel@nyu.edu

ABSTRACT

The interaction between HCN and its closely related molecule HNC, with H₂O is of considerable theoretical and experimental interest due to its important role in astrophysics^{1,2,3}. Hydrogen cyanide is one of the most observed molecules in the interstellar medium (ISM). The interpretation of HCN, and its isotope HNC, emission in comets requires the knowledge of accurate spectroscopical data and the calculation of rate coefficients for the rotational excitation of HCN and HNC by water.

In this study, we investigate the HCN-H₂O and HNC-H₂O complexes, where H₂O and HCN (or HNC) can act as proton donors or proton acceptors. We present quantum calculations for the bound-state properties of the fully coupled intermolecular rovibrational states of these van der Waals (vdW) complexes using a five-dimensional (5D) approach,^{4,5} considering the rigid-monomer approximation for total angular momentum *J* values of 0 and 1. Our analysis employs a newly developed ab initio five-dimensional potential energy surface (PES). This treatment offers a comprehensive and rigorous description

of the intermolecular rovibrational level structure of both isomers, enabling us to characterize their vibrationally averaged nonplanar ground-state geometries as well as the rotational constants of the vdW complexes. We employ two different approaches in our calculations, which vary in terms of the definition of the dimer-fixed (DF) frame and the associated coordinates. We demonstrate that using the approach introduced in this work, H₂O-HCN and HNC-H₂O exhibit unusually strong coupling, with reduced probability density plots that display signatures of simultaneous excitation in multiple internal coordinates. The calculated rotational constants show excellent agreement with experimental data. These results, along with the rotational transition frequencies, confirm that the employed PES accurately describes the rotational properties of both vdW complexes.



¹ G.J. Harris, G. J. Harris, O.L. Polyansky, J. Tennyson. *Spectrochimica Acta Part A* 58, 673–690 (2002)

² A. Heikkilä, M. Pettersson, J. Lundell, L. Khriachtchev and M. Rasanen, *J. Phys. Chem. A*, 103, 2945–2951

³ (1999) E. Quintas-Sánchez and M. L. Dubernet. *Phys. Chem. Chem. Phys.*, 19, 6849 (2017)

⁴ P. M. Felker and Z. Bačić. *Phys. Chem. Chem. Phys.*, 24, 24655–24676 (2022)

⁵ P.M. Felker and Z. Bačić. *J. Chem. Phys.* 156, 064301 (2022)

Elucidating the reaction dynamics of dissociative chemisorption of nitrogen on Ru(0001)

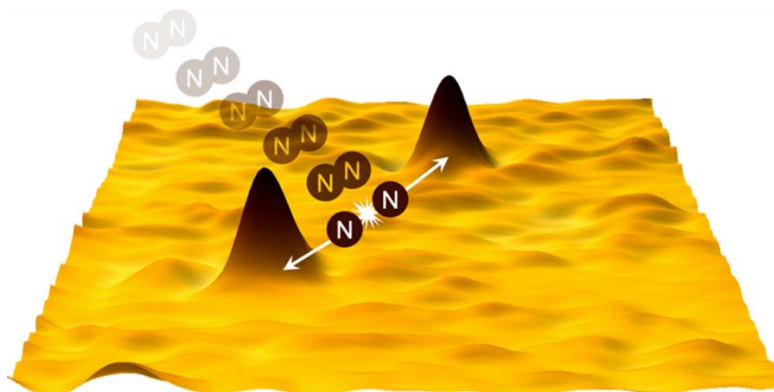
Joshua Wagner^a and Steven J. Sibener^b

^a Department of Chemistry, University of Chicago, 929 E 57th Street, Chicago, IL 60637, USA. Email: joshuawagner@uchicago.edu

^b Department of Chemistry, University of Chicago, 929 E 57th Street, Chicago, IL 60637, USA

ABSTRACT

The reactive surface dynamics of energy- and angle-selected N₂ dissociation on a clean Ru(0001) surface are analyzed through STM images showing the results of highly energetic N₂ impinging on Ru(0001) terrace sites.¹ An in situ STM in line with a supersonic molecular beam provides atomically resolved visualization of individual N₂ dissociation events to elucidate the fundamental reactive dynamics of the N₂/Ru(0001) system. The distance and angle between nitrogen atoms from the same dissociated N₂ molecule, site specificity and coordination of binding on terrace sites are precisely measured over a range of impinging N₂ kinetic energies and angles, revealing previously unattainable information about the energy dissipation channels that govern the reactivity of the system. The experimental results provide insight into the fundamental N₂ dissociation mechanism that, in conjunction with ongoing theoretical modeling,² will help determine the role of dynamical processes such as energy transfer to surface phonons and nonadiabatic excitation of electron-hole pairs (ehps).



¹ Wagner, J.; Grabnic, T.; Sibener, S. J. STM Visualization of N₂ Dissociative Chemisorption on Ru(0001) at High Impinging Kinetic Energies. *J. Phys. Chem. C* 126, 43, 18333–18342, 2022

² Wang, Y. and Guo, H. Post-dissociation Dynamics of N₂ on Ru(0001): How Far Can the “Hot” N Atoms Travel? *J. Phys. Chem. C* 127, 8, 4079–4086, 2023

Optical cycling in polyatomic molecules

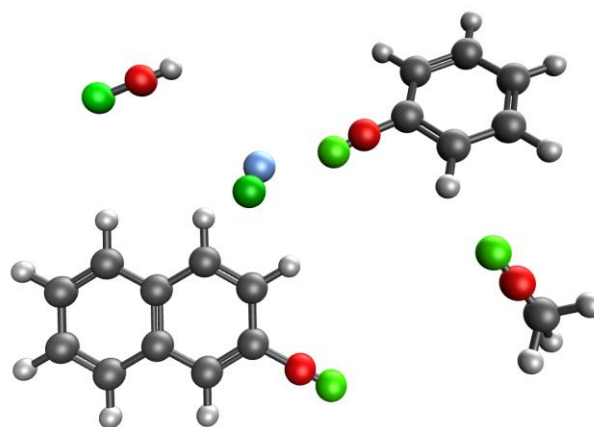
Pawel Wojcik and Anna I. Krylov

Department of Chemistry, University of Southern California, Los Angeles, California 90089, USA

Email: pawel.wojcik@usc.edu

ABSTRACT

An electronically excited state decays after a characteristic lifetime to any of the available molecular states of lower energy. The decay populates various electronic, vibrational, rotational, and spin states. Some molecules however, feature an excited state that decays almost exclusively back to the ground state. In that case a repeated laser excitation followed by spontaneous decay forms a closed optical cycle. Optical cycling on a bright transition enables rapid transfer of momentum from photons to molecules forming a basis for laser cooling. Laser-cooled molecules find applications as probes in tests of fundamental physics, hosts of a high fidelity qubits, or platforms for studying quantum state controlled chemistry.^{1–5} The first demonstration of molecular laser cooling was achieved in 2010.⁶ The breakthrough fueled more efforts in the field resulting in laser cooling of three- and six-atomic molecules in respectively 2017 and 2020.^{7,8} This progress promises optical cycling for even larger polyatomic molecules. I will present recent work from our group that focuses on exploring the domain of molecules with optical cycling centers, in particular, I will highlight applications enabled by increased chemical complexity of polyatomics.^{9–11}



<https://iopenshell.usc.edu/research/qis/>

¹ D. McCarron. Laser cooling and trapping molecules. *J. Phys. B*, 51(21):212001, 2018.

² T. A. Isaev. Direct laser cooling of molecules. *Physics-Uspekhi*, 63(3):289, 2020.

³ N. Fitch and M. Tarbutt. Laser-cooled molecules. *Adv. At. Mol. Opt. Phys.*, 70:157–262, 2021.

⁴ E. Chae. Laser cooling of molecules. *arXiv preprint arXiv:2211.13379*, 2022.

⁵ B. L. Augenbraun, L. Anderegg, C. Hallas, Z. D. Lasner, N. B. Vilas, and J. M. Doyle. Direct laser cooling of polyatomic molecules. *arXiv preprint arXiv:2302.10161*, 2023.

⁶ E. S. Shuman, J. F. Barry, and D. DeMille. Laser cooling of a diatomic molecule. *Nature*, 467(7317):820, 2010.

⁷ I. Kozryyev, L. Baum, K. Matsuda, B. L. Augenbraun, L. Anderegg, A. P. Sedlack, and J. M. Doyle. Sisyphus laser cooling of a polyatomic molecule. *Phys. Rev. Lett.*, 118(17):173201, 2017.

⁸ D. Mitra, N. B. Vilas, C. Hallas, L. Anderegg, B. L. Augenbraun, L. Baum, C. Miller, S. Raval, and J. M. Doyle. Direct laser cooling of a symmetric top molecule. *Science*, 369(6509):1366–1369, 2020.

⁹ M. V. Ivanov, F. H. Bangerter, and A. I. Krylov. Towards a rational design of laser-coolable molecules: Insights from equation-of-motion coupled-cluster calculations. *Phys. Chem. Chem. Phys.*, 21:19447–19457, 2019.

¹⁰ M. V. Ivanov, S. Gulania, and A. I. Krylov. Two cycling centers in one molecule: Communication by through-bond interactions and entanglement of the unpaired electrons. *J. Phys. Chem. Lett.*, 11(4):1297–1304, 2020.

¹¹ M. V. Ivanov, F. H. Bangerter, P. Wójcik, and A. I. Krylov. Towards ultracold organic chemistry: Prospects of laser cooling large organic molecules. *J. Phys. Chem. Lett.*, 11:6670–6676, 2020.

Gas-Phase Formation of the Resonantly Stabilized 1-Indenyl ($C_9H_7^\bullet$) Radical in the Interstellar Medium

Zhenghai Yang,^a Galiya R. Galimova,^b Chao He,^a Shane J. Goettl,^a Dababrata Paul,^a
Wenchao Lu,^c Musahid Ahmed,^c Alexander M. Mebel,^b Xiaohu Li,^{d,e} and Ralf I. Kaiser^a

^a *Department of Chemistry, University of Hawai'i at Manoa, Honolulu, Hawaii 96822, USA*
Email: zyang@hawaii.edu

^b *Department of Chemistry and Biochemistry, Florida International University, Miami, Florida 33199, USA*

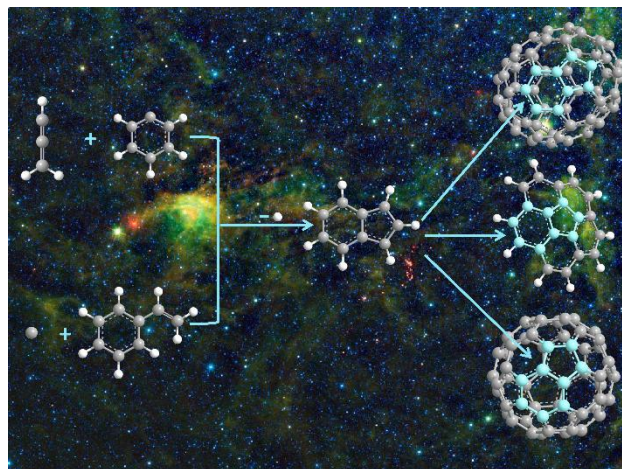
^c *Chemical Sciences Division, Lawrence Berkeley National Laboratory, Berkeley, CA 94720, USA*

^d *Xinjiang Astronomical Observatory, Chinese Academy of Sciences, Urumqi, Xinjiang 830011, P. R. China*

^e *Key Laboratory of Radio Astronomy, Chinese Academy of Sciences, Urumqi, Xinjiang 830011, P. R. China*

ABSTRACT

The 1-indenyl ($C_9H_7^\bullet$) radical - a prototype aromatic and resonantly stabilized free radical (RSFR) carrying a six- and a five-membered ring - has emerged as a fundamental molecular building block of non-planar polycyclic aromatic hydrocarbons (PAHs) and of carbonaceous nanostructures in deep space and in combustion systems. However, the underlying elementary mechanisms of formation of 1-indenyl in these extreme environments have remained largely elusive. Here, we reveal an unconventional low-temperature gas-phase formation of 1-indenyl ($C_9H_7^\bullet$) via barrierless ring annulation involving reactions of atomic carbon ($C(^3P)$) with styrene ($C_6H_5C_2H_3$) and of the propargyl radical ($C_3H_3^\bullet$) with the phenyl radical ($C_6H_5^\bullet$). Macroscopic environments like molecular clouds act as natural low-temperature laboratories, in which rapid molecular mass growth processes to interstellar 1-indenyl and subsequently to more complex PAHs involving vinyl side-chained aromatics and aromatic aryl radicals can occur. This sequence of reactions and versatile mechanism to prepare aromatic RSFRs under the extreme low temperature conditions in molecular clouds might augment PAH production in deep space thus explaining the presence of PAHs along with their derivatives in the interstellar medium and carbonaceous chondrites and closing the gap of timescales of their production and destruction in our Universe.



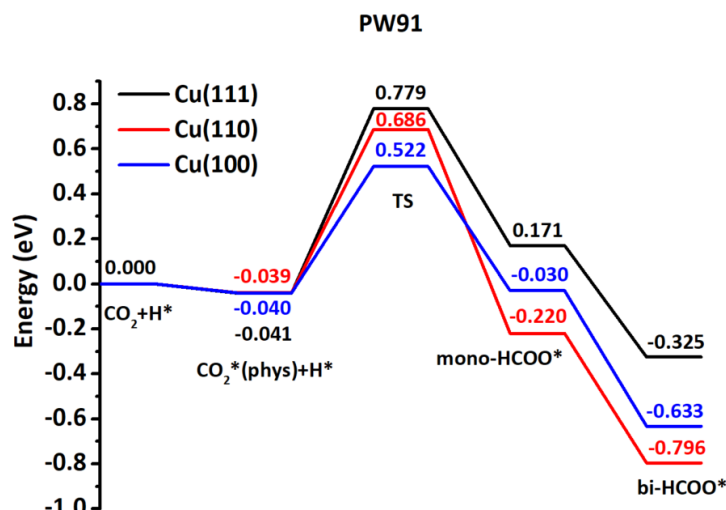
Theoretical Study of Formate Decomposition on Cu Catalysts

Rongrong Yin and Hua Guo

Department of Chemistry and Chemical Biology, University of New Mexico, Albuquerque,
NM 87131, USA. Email: yinrrch666@unm.edu

ABSTRACT

In this work, *ab initio* molecular dynamics (AIMD) calculations based on density functional theory (DFT) have been carried out to understand the post-transition state dynamics for formate (HCOO) decomposition on three model surfaces of Cu — Cu(111), Cu(110) and Cu(100). Formate, which is an important reaction intermediate in many catalytical processes, is known to adsorb with a bidentate configuration. Its decomposition proceeds to the conversion to a mono-dentate configuration, followed by the cleaving of the H-C bond. Our AIMD simulations showed that the CO₂ product is translationally hot with angular distributions sharply collimated along surface normal, in agreement with experimental measurements.¹ Furthermore, the CO₂ product was found to have rotational and vibrational excitations, mostly in the bending mode.² These product state distributions are rationalized by the Sudden Vector Projection model,³ revealing the key role of the transition state in product energy disposal. Specifically, the CO₂ bending excitation originates from the bent geometry at the decomposition transition state.



¹ Quan, J.; Kondo, T.; Wang, G.; Nakamura, J. J. A. C., Energy Transfer Dynamics of Formate Decomposition on Cu (110). *Angew. Chem. Int. Ed.*, 13 (129), 3550-3554, 2017.

² Quan, J.; Muttaqien, F.; Kondo, T.; Kozarashi, T.; Mogi, T.; Imabayashi, T.; Hamamoto, Y.; Inagaki, K.; Hamada, I.; Morikawa, Y.; Nakamura, J., Vibration-driven reaction of CO₂ on Cu surfaces via Eley–Rideal-type mechanism. *Nature Chemistry*, 11 (8), 722-729, 2019

³ Jiang, B.; Guo, H., Relative Efficacy of Vibrational vs. Translational Excitation in Promoting Atom-Diatom Reactivity: Rigorous Examination of Polanyi's Rules and Proposition of Sudden Vector Projection (SVP) Model. *J. Chem. Phys.* 138, 234104, 2013.

Product angular distribution in the $\text{H} + \text{CD}_4 \rightarrow \text{HD} + \text{CD}_3$ reaction

Bin Zhao,^{1,2} Uwe Manthe,² Donghui Zhang¹

¹Department of Chemistry, Southern University of Science and Technology, Shenzhen 518055, People's Republic of China. Email: zhaobin@sustech.edu.cn

²Theoretische Chemie, Fakultät für Chemie, Universität Bielefeld, Bielefeld 33615, Germany

ABSTRACT

First-principles based study of quantum state-to-state reaction dynamics aims to provide insights into the most detailed dynamical processes of chemical reactions and has achieved great success in predicting and explaining fascinating quantum effects in various tri-atomic systems. This field has now advanced to polyatomic reaction systems, and reactions of CH_4 with various atoms are the most studied systems.

Recently, counterintuitive effects are found in the $\text{H} + \text{CHD}_3 \rightarrow \text{H}_2 + \text{CD}_3$ reaction:¹ Increasing the energy in the reactant's CD_3 umbrella vibration reduces the energy in the corresponding product vibration. An in-depth analysis reveals the crucial role of the effective dynamical transition state: Its geometry is controlled by the vibrational states of the reactants and subsequently controls the quantum state distribution of the products.

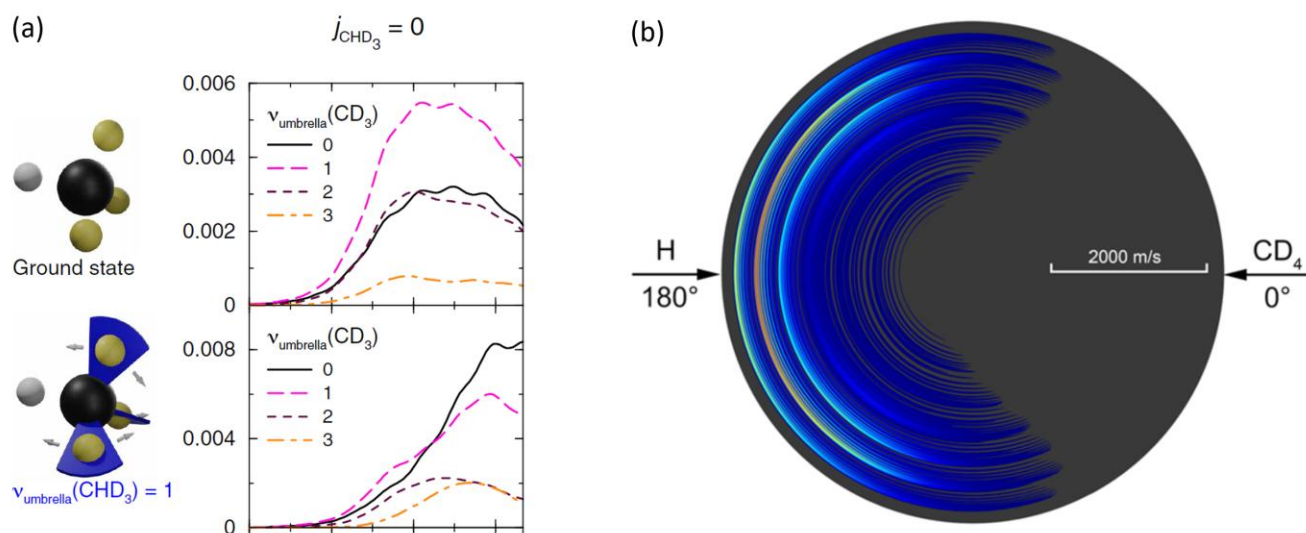


Figure. (a) Counterintuitive CD_3 umbrella vibrational excitation in the $\text{H} + \text{CHD}_3 \rightarrow \text{H}_2 + \text{CD}_3$ reaction; (b) The velocity and angle-resolved state-specific differential cross sections of the $\text{H} + \text{CD}_4 \rightarrow \text{HD} + \text{CD}_3$ reaction at a collision energy of 0.72 eV.

Very recently, we performed a theoretical study of the $\text{H} + \text{CD}_4 \rightarrow \text{HD} + \text{CD}_3$ reaction² with the time-dependent wave packet method using a seven-dimensional model Hamiltonian developed by Palma and Clary. The velocity and angle-resolved state-specific differential cross sections (DCSs) at a collision energy of 0.72 eV are investigated in detail. Two detection schemes based on measuring the state-selective $\text{HD}(v_1, j_1)$ and $\text{CD}_3(v_2, j_2)$ products are compared. The very interesting angular distribution of the CD_3 product is explained with the concept of the effective dynamical transition state.

¹ R. Ellerbrock, B. Zhao, U. Manthe, Sci. Adv. 8, eabm9820 (2022)

² in preparation

The persistent $l = \text{even}$ feature of the $\text{D}_2\text{-Rg(He,Ne)} \Delta j = 2$ scattering?

Haowen Zhou, William Perreault, Nandini Mukherjee, and Richard Zare

Department of Chemistry, Stanford University, CA 94305, USA. Email: hwzhou@stanford.edu

ABSTRACT

Low-energy collisions are important to understand molecular interactions. In particular, dynamics of a scattering resonance is sensitive to the shape of the potential energy surface, hence providing the most detailed probe. In the past few years, we have conducted a series of $\Delta j = 2$ rotationally inelastic scattering between rovibrationally excited D_2 ($v = 2, 4, j = 2$) molecules with rare gas atoms He, Ne at cold temperatures ~ 1 K. Despite the different vibrational levels and different collision partners involved, we have repeatedly discovered similar $l = \text{even}$ features by fitting the product angular distributions using partial wave analysis. These features are consistent between various collision geometries, which we attribute to the $l = 2$ resonance of the collision complex.^{1,2}

However, our experimental findings do not agree well with theory. For $\text{D}_2\text{-He}$, previous theoretical calculations³ have identified a more predominant $l = 1$ resonance in our collision temperature range. There are less works on $\text{D}_2\text{-Ne}$, but an earlier spectroscopic measurement⁴ found an $l = 5$ resonance complex. But since both resonances are $l = \text{odd}$, they would result in completely different scattering angular distributions than the experiment.

We are currently looking for the cause of this discrepancy. In an intrabeam setup, cold collisions are realized between the faster and slower velocities in a single molecular beam. This poses a challenge in defining the collision energy. Detailed characterization should be further performed for the coexpansion process. But in general, the dominance of a single partial wave and the similarity across different scattering partners seem to indicate a common feature in our current experimental setup which has not been identified.

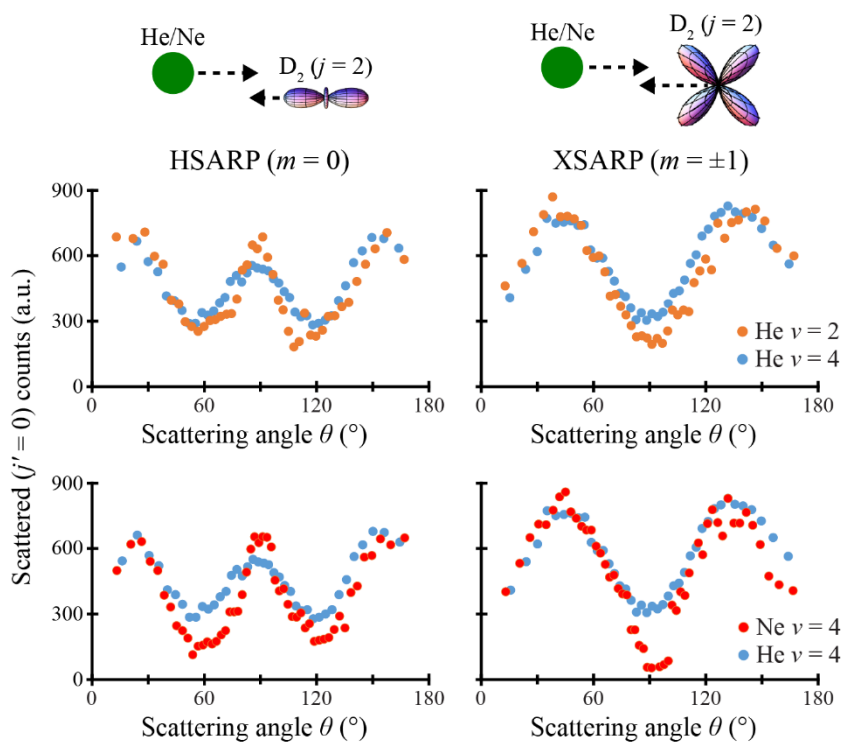


Figure 1. Comparison between the scattering angular distributions for $\text{D}_2(v = 2)$ and $(v = 4)$ with He (top), and $\text{D}_2(v = 4)$ with He and Ne (bottom). Two different alignments ($m = 0$) and ($m = \pm 1$) are presented. All distributions are normalized to the same height.

¹ Zhou, H., Perreault, W. E., Mukherjee, N. & Zare, R. N. Shape resonance determined from angular distribution in $\text{D}_2(v = 2, j = 2) + \text{He} \rightarrow \text{D}_2(v = 2, j = 0) + \text{He}$ cold scattering. *J. Chem. Phys.* **154**, 104309 (2021).

² Perreault, W. E., Zhou, H., Mukherjee, N. & Zare, R. N. Resonant cold scattering of highly vibrationally excited D_2 with Ne. *J. Chem. Phys.* **157**, 144301 (2022).

³ Jambrina, P. G., Morita, M., Croft, J. F. E., Aoiz, F. J. & Balakrishnan, N. Role of Low Energy Resonances in the Stereodynamics of Cold $\text{He} + \text{D}_2$ Collisions. *J. Phys. Chem. Lett.* **13**, 4064–4072 (2022).

⁴ McKellar, A. R. W. High-resolution infrared spectra of $\text{H}_2\text{-Ne}$ and $\text{D}_2\text{-Ne}$ van der Waals complexes. *Can. J. Phys.* **87**, 411–416 (2009).